2008

Self-healing of impact-damaged composites

Louis Henry Charles
Iowa State University

Self-healing of impact-damaged composites

by

Louis Henry Charles

A thesis submitted to the graduate faculty

in partial fulfillment of the requirements for the degree of

MASTER OF SCIENCE

Major: Materials Science and Engineering

Program of Study Committee:
Michael R. Kessler, Major Professor
Zhiqun Lin
Vinay Dayal

Iowa State University

Ames, Iowa

2008

TABLE OF CONTENTS

LIST OF FIGURES

LIST OF TABLES

ACKNOWLEDGEMENTS

I extend my gratitude to: Dr. Michael Kessler for his guidance and background in the self healing system, Tim Mauldin for sharing his counsel and expertise in both the theory and practice of the microcapsules and the HTDCB specimens, Dr. Will Goertzen, Dr. Xia Sheng, Wonje Jeong, Xing Liu, Dr. Jong Keun Lee, Fen Chao for aiding me through the obstacles of testing and lab equipment; Nate Marsen, Ben McMurray, Cory Sents, Dan Putnam, and Charlotte Mok for help with sample preparation and testing, and Dick Egger, Terry Soseman and Bruce Erickson in the Chemistry Machine Shop for help in creating molds, cutting samples, and having the right tools for the job. I especially thank my wonderful wife Jessie for her encouragement and support, and much needed common-sense advice.

ABSTRACT

Extensive work in the field of self-healing materials has developed several different methodologies and multiple successful systems utilizing the various approaches. Within the paradigm of healing using an embedded microencapsulated healing agent and catalyst the specific materials used can greatly influence the healing efficiency of the system. This work compares the adhesive capabilities of a number of ROMP-capable healing agent candidates. The success of the system at healing Mode I damage in fiber-reinforced composites (FRC) has been demonstrated. This work applies that same self-healing system to the mixed mode failure that occurs from impact damage of a FRC. While the system still allows the necessary steps for self-healing to occur, the damage suffered by this system was more extensive than the repair capabilities of the healing system.

CHAPTER 1: GENERAL INTRODUCTION

1.1 Introduction

Composites have long been valued for their ability to combine the advantageous properties of different materials. There is a high demand currently for materials that not only combine various properties but can combine various roles. These 'multi-functional' materials might be both a structural material and an actuator or a protective coating and a sensor. Significant interest exists in developing structural materials that also have the ability to self-heal.

1.2 Dissertation organization

This work is organized into four chapters. Chapter 1 provides the general introduction to and overview of different self-healing approaches. It details the background of what has been developed and investigated for one methodology – the use of microencapsulated healing agents, which explains the motivations for the present work. This chapter also explains the reasons and theory behind the tapered double-cantilever beam specimens used for the first objective. An introduction to the studying of impact damage of composites is also provided.

Chapter 2 addresses the comparison of different healing agent candidates. The adhesive capability of endo-DCPD is compared to exo-DCPD, endo-exo DCPD blends, ENB, and ROMP monomers with crosslinking agents and other additives.

Chapter 3 considers the applicability of the present self-healing system to the healing of impact damage in fiber-reinforced composites. The difficulties and challenges of producing and comparing damage are discussed.

Chapter 4 gives the general discussion of how these efforts have contributed to the knowledge of the self-healing system. It also includes recommendations for future work.

1.3 Background and literature review

1.3.1 Current Self-Healing Approaches

Just as there are a wide variety of ways for a sample to fail, there are several different approaches to self-healing. The three main approaches in the literature are thermally-activated solid-phase healing, healing of projectile punctures, and healing through an embedded liquid-phase healing agent [1]-[3].

1.3.1.1 Thermally-Activated Solid-Phase Healing

At least two different approaches utilize external heating to mend polymer fractures. Both Chen et al [4]]-[[5] and Plaisted [6] et al have demonstrated healing in a polymer system that utilizes a thermally reversible Diels-Alder reaction and retro-Diels-Alder cycloaddition. These polymers consist of a mulifuran molecule combined with a multimaleimide molecule in various stoichiometric ratios. Not all the bonds in the polymer chain are healable: the system has been designed such that the weaker bonds that will preferentially break under load are those that can undergo the reaction when subjected to

external heat. When the fracture surfaces are brought back into contact and the heat necessary for reaction is applied, the bonds are able to reform.

Hayes et al [7] have developed a system that, while it also relies on external heat, utilizes a different method for rebonding the crack faces. This system consists of a thermoset epoxy matrix, within which a linear thermoplastic is dissolved. At lower temperatures the thermoplastic "healing agent" is held in the matrix by hydrogen bonding, but as the temperature increases it becomes free to interdiffuse throughout the matrix. The matrix itself is not healing, but the thermoplastic can self-transport and bridge the gap. While both of these systems have shown promising healing efficiencies, neither is truly autonomic *self*-healing, as external heat is required.

1.3.1.2 Projectile Puncture

One application with immense potential benefit from self-healing is projectile punctures. Kalista et al [8] have investigated a copolymer, poly(ethylene-*co*-methacrylic acid) (EMAA), that has demonstrated the ability to reclose and seal off projectile punctures in a film. EMAA is an ionomer and it was initially assumed that the ionic nature of the polymer was the significant factor in the healing behavior. Further investigations have indicated that non-ionic forms of these copolymers still heal, and increasing the ionic nature is more detriment than aid. More recent work has shown that it is the localized viscoelastic melting that allows the material around the hole to elastically rebound to close the hole and that the polymer chains interdiffuse to allow the region to seal off. The temperature increase, projectile geometry, and timing are critical to successful healing. In addition to ballistic puncture, the heat generated by sawing is sufficient for the material to

rebond. Cutting does not produce enough heat, and a puncture which removes material or in which the object remains in the film cannot be healed.

1.3.1.3 Embedded Liquid-Phase Healing Agent

Self-healing ability through the use of a liquid-phase healing agent depends on four basic criteria. First, the healing agent must be stored within the composite. Second, it must be released from the storage mechanism. Third, it must be able to transport itself from the initial storage location to the crack plane. Fourth, it must rebond the crack surfaces. Within each criterion (storage, release, transport, and rebonding) a variety of factors influence the efficiency of the system as a whole [1].

Healing Agent Within Fiber Reinforcement

One approach to embed the liquid phase healing agent is to use hollow tubes or fibers as the storage mechanism. While hollow glass fibers result in a composite with somewhat reduced strength capabilities compared to solid fibers, their response to impact damage is comparable. Hollow glass fibers have a significantly larger outer diameter than the solid glass fibers typically used in a GFRC. When used, the hollow fibers are not the only structural reinforcement, but are scattered in with the solid fibers. This approach has shown promise, as it addresses the four healing criteria well. Storing the healing agent inside the fibers allows for good distribution throughout the composite. When damage occurs it is the storage fibers that break, releasing the healing agent at the break location, which minimizes the transport distance. Because most impact damage is localized, it is advantageous to have the broken fiber contain healing agent not only in the localized

region. Each broken fiber has a 'reservoir' of healing agent – the undamaged areas from which it can draw more healing agent to make sure the entire crack volume can be filled. To achieve polymerization the resin released from the hollow fibers must come into contact either with a hardener similarly embedded in separate hollow fibers or with a microencapsulated catalyst or hardener as seen in Figure 1 [9]-[12].

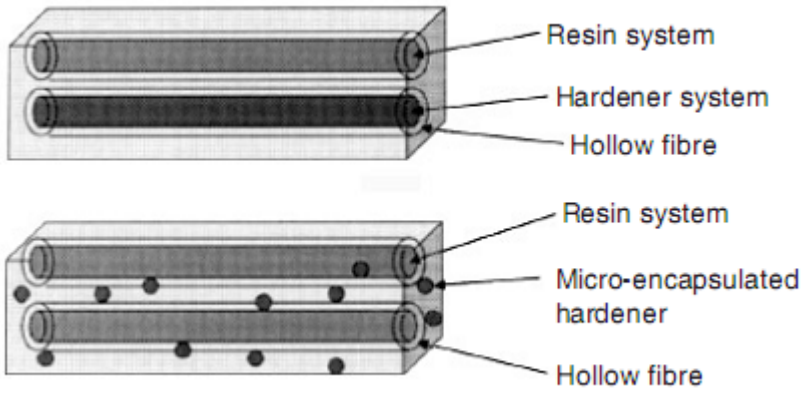

Figure 1: Schematic illustration of different hollow fiber self-healing approaches

Another similar approach is a system developed by Toohey et al [13] wherein a 3-D network of hollow interconnected channels, a 'micro-vascular network', contains the healing agent. When the strain causes a rupture anywhere in the network the healing agent is transported out of the network and into the crack plane by capillary action. One positive feature of this approach is that when a crack releases the healing agent, there is an ample supply of healing agent, as the fluid from the entire network is available to move to the damage site.

Microencapsulated Healing Agent

Since the groundbreaking work by White et al [14] several groups have been developed and advanced self-healing by means of a microencapsulated liquid healing agent. A schematic of how self-healing utilizing microcapsules is shown in Figure 2. Storage of a healing agent involves both encasing and distributing the microcapsules and catalyst throughout the composite. Successful storage results in microcapsules that are well-distributed, stable enough to protect both the healing agent and catalyst from reaction with the matrix, and sturdy enough to not rupture during composite fabrication.

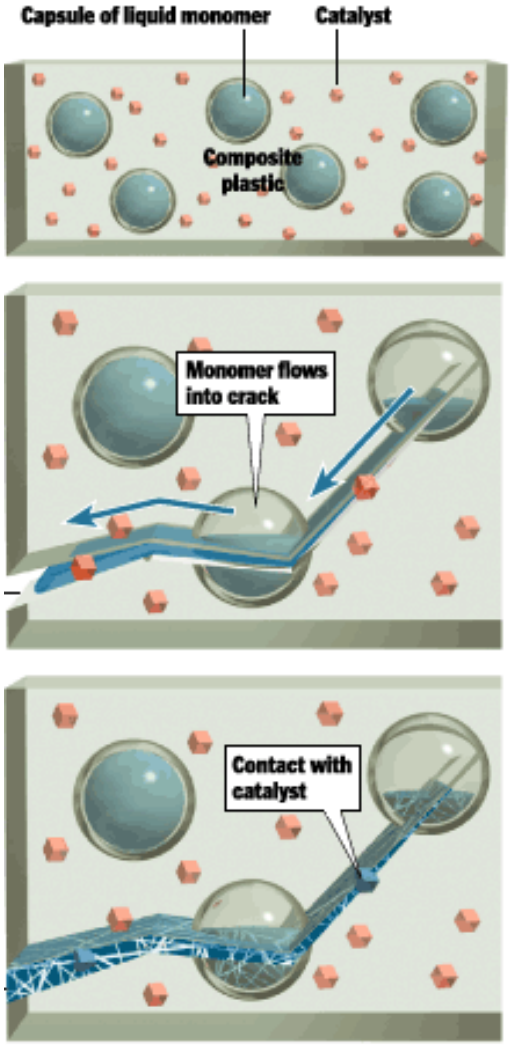

Figure 2: Self-healing with microcapsules: Storage, release, transport and rebonding

The capsules cannot be too tough, however, lest they interfere with the release stage. Successful release will only occur as capsules are split by the growing crack. Other events (i.e. manufacturing process, thermal or chemical degradation) must not cause capsule failure. Capsules that are too tough will not open with the widening crack and will pull out of the matrix intact and useless.

Storage and release are largely dependent on the chemical and mechanical behavior of the microcapsules, while transport and rebonding depend on the properties of the healing agent and catalyst. The driving force for transport of the healing agent along the crack surfaces is capillary action. For effective transport the healing agent must have a lower surface energy than the newly exposed crack faces to encourage wetting into as much of the crack volume as possible. The transport stage also includes bringing the healing agent and catalyst into contact with each other.

Contact between the catalyst and healing agent triggers the polymerization that rebonds the crack faces together. This 'gluing' of the crack faces redistributes the stress concentration away from crack tip across much more of the crack length. Successful rebonding consists of strong adhesion of the polymerized healing agent to the crack plane and high cohesive strength within the healing agent. Additionally, the polymerization step should occur rapidly, but not so quickly that the monomer is unable to spread throughout the crack plane. Too swift polymerization in a small region immediately surrounding the catalyst might also prevent the catalyst from being sufficiently dissolved, effectively encapsulating the catalyst and leaving uncured monomer.

The early work by White et al [14] utilized a class of monomers capable of undergoing ring-opening metathesis polymerization (ROMP) as the healing agent, primarily dicyclopentadiene (DCPD) polymerized using Grubbs' Catalyst [15], but other systems have been developed as well. Cho et al [16] developed a system based on polydimethylsiloxane (PDMS), while Yin et al [17] have demonstrated healing in a system in which it is epoxy acting both as the matrix and as the curing agent. Several studies have taken the

methodology developed by White and colleagues and sought to either improve the healing efficiency of the system or further the understanding of any of the four critical stages [36][37].

STORAGE

Microcapsules

Significant effort has been directed towards quantifying and enhancing microcapsule performance. The microcapsules themselves are produced when the monomer healing agent is separated into micro-sized droplets in an oil-in-water emulsion. The capsule components then polymerize at the high-energy interface, growing the shell around the monomer. Processing conditions such as time, temperature, pH, and agitation rate control the sphere diameter, size distribution, shell thickness, surface texture, strength, and permeability of the capsules. Proper drying strongly influences the ability of the microcapsules to flow well and not agglomerate in processing. An early successful processing method is described in [18].

One of the most easily adjusted and most critical parameters is sphere diameter, which is controlled by changing the agitation rate [19]. For comparable shell thicknesses, larger capsules have the advantages of holding a greater volume of healing agent in each capsule as well as a larger fraction of the total capsule weight consisting of healing agent rather than capsule wall. Larger capsules are subjected to greater shear forces in processing. In addition, large capsules would almost certainly be destroyed by any pressure normal to the plies of a fiber-reinforced composite. Smaller capsules ideally allow for a

more equal distribution throughout the matrix increasing the likelihood that any given crack will encounter a microcapsule. Rule et al examined the effect of microcapsule size on healing efficiency and found that there is an optimum size for a given system that will result in the best possible healing efficiency. Capsules larger than that size do not demonstrate any further advantage [20]. Blaiszik et al have recently demonstrated effective encapsulation of monomer into nano-sized capsules using ultrasonic processing methods [21]. The healing potential of such nanocapsules would almost certainly be diminished by the minute quantity of healing agent contained within each capsule. Further, since a much greater weight fraction of each nanocapsule is shell wall, significantly higher loading would be required to embed the same amount of healing agent into the composite.

Increasing the surface roughness of the capsules provides an increase in area for adhesion as well as greater potential for mechanical interlocking between the shell wall and the matrix. Improving the adhesion between the microcapsule shell and the surrounding matrix increases the likelihood that an advancing matrix crack would also rupture the microcapsule. Other processing conditions can produce capsules that have the appearance of spheres with substantial bits of debris on the outside of the shell. This debris adds to the weight without adding healing potential and if it is not adhered well to the capsule surface might in theory behave as a release agent separating the microcapsules from the matrix intact.

Microcapsules have been successfully fabricated with different compositions for the capsule wall. Reference [18] describes a pathway to produce poly (urea-formaldehyde) (UF) microcapsules. Liu and Lee demonstrated that with the addition of melamine poly

(melamine-urea-formaldehyde) (MUF) microcapsules could be produced with excellent uniformity, roundness, and minimal surface debris [22]. In contrast with UF microcapsules MUF capsule processing does not require adjusting the pH of the emulsion. One of the most important aspects of the shell is its durability. Keller and Sotos developed a method for quantifying the mechanical strength of the microcapsules [23]. In addition to mechanical durability, there are concerns over shelf-life for microencapsulated monomers. Empirical evidence has shown a tendency in some systems for the monomer to leach out of the capsule with time during extended storage. Microcapsules that leak loose monomer and therefore healing effectiveness with time. Additionally, the liquid that has leached out causes the adjacent capsules to clump together, resulting in poorer distribution throughout the matrix and an easier failure path, separating rather than rupturing capsules. Ideal capsules should have a long shelf life, allowing for producing larger batches than can be used at a future date without degradation in properties [24].

Extra care must be taken with any adjustments to the 'healing agent' composition. Additives to the monomer may also require special processing to produce high-quality capsules. Everything from crosslinking agents [25] to carbon nanotubes can change the properties of the 'healing agent' in ways that necessitate processing adjustments. Viscosity, pH, surface energy and more can change; additives can settle or agglomerate; additives may react chemically with the microcapsule materials or may change with the heat and acidity of the environment.

Catalyst

Ring-opening metathesis polymerization (ROMP) requires a catalyst to convert the monomers into the network of chains and crosslinks that makes such polymers good self-healing candidates. The most effective, and therefore, commonly used are a family of ruthenium-based Grubbs' catalysts [15]. While there are several varieties of Grubbs' catalyst, they are all prohibitively expensive. Considerable effort has gone into minimizing the amount of Grubbs' catalyst required while still delivering optimum healing performance. One of the challenges to be overcome is that Grubbs' catalyst reacts with the primary amines that are frequently used as curing agents for the epoxy matrix, decreasing catalyst effectiveness. Further, smaller catalyst morphologies that improve ROMP kinetics leave the catalyst more susceptible to degradation by the epoxy curing agent.

Taber *et al* developed a method of protecting Grubbs' catalyst in paraffin wax microspheres for use in other systems [26]. Rule *et al* applied these lessons to the self-healing system [27]. Wax encapsulation provides important storage benefits while not impeding release or rebonding. The catalyst is protected from the amine curing agent by the wax, which readily dissolves in the DCPD, allowing the monomer and catalyst to mix. Wax microspheres also allow for better distribution of the catalyst throughout the matrix. Unprotected Grubbs' catalyst has a tendency to agglomerate, resulting in many regions without adequate catalyst and a few regions with more catalyst than is needed by the amount of monomer present. This makes it less likely that healing agent in a crack growing at random will encounter the needed catalyst, which in turn, increased the amount of

catalyst required to achieve comparable healing. An overabundance of catalyst can also lead to too-rapid polymerization. The fraction of catalyst in the wax can be adjusted for optimum efficiency as can the sphere size.

RELEASE

Most of the factors that influence release of the healing agent and catalyst into the crack plane are controlled by processing during the storage phase. Of first importance, the monomer must not release prior to the damage event, neither before nor during processing. A delicate processing balance must be made to produce capsules with walls thick enough to prevent diffusion of the monomer and rupture during processing while also being thin enough to fail during the damage event. The shell wall should have sufficient adhesion to the surrounding matrix that when a crack opens in the matrix the capsule walls deflect enough to rupture/tear. Any chemical or mechanical means of increasing adhesion between the shell wall and the surrounding matrix will help ensure that all capsules in the crack plane do release their contents at the right time. Ideal sphere release would leave the capsules torn cleanly along the crack plane with no pullout from the matrix. Capsules with a tendency toward pull-out will be less likely to rupture the farther from center the crack encounters the sphere [24].

Release of the catalyst is entirely dependent on the ability of the healing agent to reach and dissolve the wax. One parameter for comparing the effectiveness of different healing agent candidates is the rate of dissolution of the protective wax. It has been hypothesized that adding a small amount of solvent to the healing agent within the

microcapsules could increase the rate of dissolution of the wax and/or the rate of dissolution of the catalyst.

TRANSPORT

The primary mechanism for transport of the healing into the crack plane is capillary action. As such smaller cracks, especially microcracks, have greater potential for healing for a variety of reasons. Capillary forces are greater in smaller channels – providing stronger wicking action to pull the healing agent throughout the extent of the interconnected cracks. Here the microcapsule system is at a disadvantage compared to either a lattice network or the hollow fiber approach. Only microcapsules in the crack plane can empty their healing agent into that plane. Other systems can draw upon the healing agent in the undamaged regions to provide sufficient healing material to fill the crack volume. Larger cracks have a significantly greater volume which means a drastic increase in the quantity of healing agent that must be present to fill the void. Too large a crack might effectively release the healing agent from the microcapsule but create a gap between crack faces so large that the volume released can fill only a small fraction of the crack volume. It could leave the released healing agent in a high-strength polymerized state but only touching one crack face and therefore useless. In such a case even if the monomer was close enough to a catalyst sphere and could dissolve the wax it could polymerize without any benefit at all as it would not be binding the two faces together. As such a system in which the cracks were somehow compressed or closed after the damage event would have more effective transport. Ideally the crack displacement should be significantly less than the diameter of the microcapsules –

roughly an order of magnitude less or even smaller. In the case of the aforementioned nanocapsules all but the smallest microcracks would cause a gap so wide that even if the crack faces were lined with ruptured capsules the volume would be insufficient to bridge the chasm.

Lower viscosity corresponds to easier flow. Conditions which create a more favorable surface energy situation can also improve transport. The lower the surface energy of the healing agent as compared to the fracture surface the more the system wants to wet and spread across the crack plane. If the cracks connect with the surface of the composite (highly likely in the case of impact damage) the liquid must not all pull out of the crack plane or evaporate before it can polymerize [24].

REBONDING

After the healing agent has been released from the microcapsules and transported throughout the crack plane, to effect healing it must polymerize and 'glue' the crack faces together. This rebonding creates a much greater area on which the crack opening force must act, greatly reducing the stress concentration at the crack tip. In general this involves the reaction of the healing agent with a catalyst or triggering agent that has also been embedded within the matrix and is mixed *in situ*. To be truly self-healing this reaction should occur at room temperature. The reaction should occur quickly enough that the bulk material does not suffer further damage before the polymerization and damage resistance has taken effect.

The majority of research since White's initial paper demonstrating this type of healing [14] has focused on the rebonding stage [28]-[32]. Rebonding is dependent on several factors relating to the healing agent, the catalyst, the matrix, environmental conditions, damage modes, etc. Slugovc's review of numerous ROMP systems is an excellent guide to potential ROMP healing agents, catalysts, and the conditions under which different combinations might be favorable [33]. One major factor in polymerization kinetics is the size and morphology of the catalyst particles. Catalyst particle size, in conjunction with agitation speed during processing, control the wax particle size. The catalyst particle size and morphology can vary from supplier to supplier, but can be controlled either by mechanical grinding, dissolution in a solvent and recrystallization, or by freeze drying. Smaller particles are more easily dissolved into the monomer and therefore cause a faster reaction. At the same time, the smaller particles are more likely to react with the matrix hardener and lose effectiveness. Jones et al examined the effect of catalyst morphology on the dissolution kinetics for DCPD [34].

1.3.2 Tapered Double-Cantilever Beam Specimens

Since the essential role of the healing agent in such a system is as an adhesive bonding the two crack faces together, comparing different healing agent/catalyst combinations is basically a comparison between adhesives. One of the most useful parameters in comparing adhesives is the strength in Mode I stress. The standard sample for measuring Mode I stress intensity factor is the edge crack compact tension specimen.

The standard equation to calculate the Mode I stress intensity factor (K_I) of an edge crack compact tension specimen $K_I = \sigma_{yy}^{\infty}\sqrt{\pi a}$ requires that the stress, σ (load and uncracked area), and the crack length (a) at a given time are known. Such tests produce a continuously increasing stress intensity factor as the crack advances. As the crack grows it may be difficult to measure or record the precise crack length for a given load. Under such conditions it can be impossible to isolate the dependence of results to microstructure, environment, temperature, etc. For such cases a specimen with a constant K value has been developed by altering the geometry such that the ratio of crack length a to beam height h remains constant as the crack grows: a tapered double-cantilever beam (TDCB) [43]. A major advantage of the TDCB specimen is that the critical fracture toughness K_{IC} is directly proportional to the critical load P_C. This allows for an easy comparison between the K_{IC} for different conditions simply by comparing the failure load. TDCB samples are generally much smaller than compact tension specimens [43].

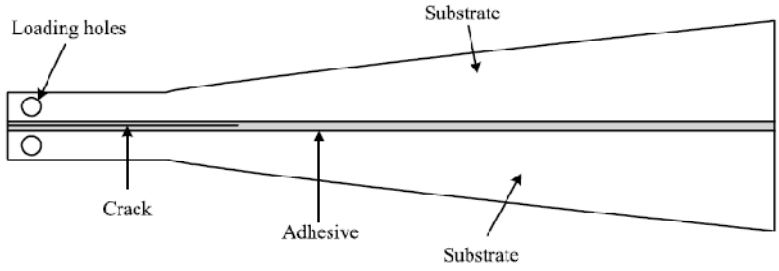

Figure 3: The TDCB adhesive joint specimen

Tapered double-cantilever beam samples are also very useful for calculating the Mode I energy release rate G_I for the same reason as above – namely the independence from crack

length. The Irwin-Kies equation defines the energy release rate *G* as the rate of change of potential energy with respect to the crack extension area:

$$G_{IC} = \frac{P^2}{2b}\frac{dC}{da}$$

where *P* is the applied load, *b* the specimen width, *C* the specimen compliance and *a* the crack length. *C* is defined as displacement divided by load. d*C*/d*a* was defined by for a uniform DCB as:

$$\frac{dC}{da} = \frac{8}{Eb}\left(\frac{3a^2}{h^3} + \frac{1}{h}\right) \qquad m = \frac{3a^2}{h^3} + \frac{1}{h} \qquad \text{hence} \quad G_I = \frac{4P^2}{Eb^2}(m)$$

where E is the modulus and h the height. The term in the parenthesis is defined as the geometry term *m*, with the 1/h representing the effect of shear deformation and the other term as representing the effect of bending deformation. Studies have been done showing that the effects of shear deformation are small compared to bending and the 1/h term is usually dropped. Some attempts have been made to refine the governing equations for the TDCB specimen, and while they have shown a slightly more accurate fit the general case works well [45].

Since the stress intensity factor and energy release rate are constant for the tapered system, comparing healing efficiency (η) can be accomplished simply by comparing the critical fracture loads (P_C) prior to the failure event (P_C Virgin) and after healing (P_C healed) [44]:

$$\eta\ (\%) = \frac{P_C^{healed}}{P_C^{virgin}} \times 100$$

1.3.3 Impact and Compression After Impact of Composites

One of the biggest threats to fiber-reinforced composite structures, particularly in the aerospace industry, is impact damage. A distinction is generally made between high-velocity impact (ballistic or projectile type) and low-velocity impact (hail, dropped tools, etc.) with the threshold at 20 m/s (44.7 mph) [54]. This work deals exclusively with low velocity impact. Low velocity impact poses an acute threat to these types of structures because the bulk of the damage caused is sub-surface and may never be visually apparent from the impact site. This internal damage can significantly reduce the capability of the structure, particularly in compression. Such damage is typically noted as barely visible impact damage (BVID). The Federal Aviation Administration requires that all composite structures have sufficiently high safety factor that even in the event of BVID the part not be reduced below the design ultimate load [64].

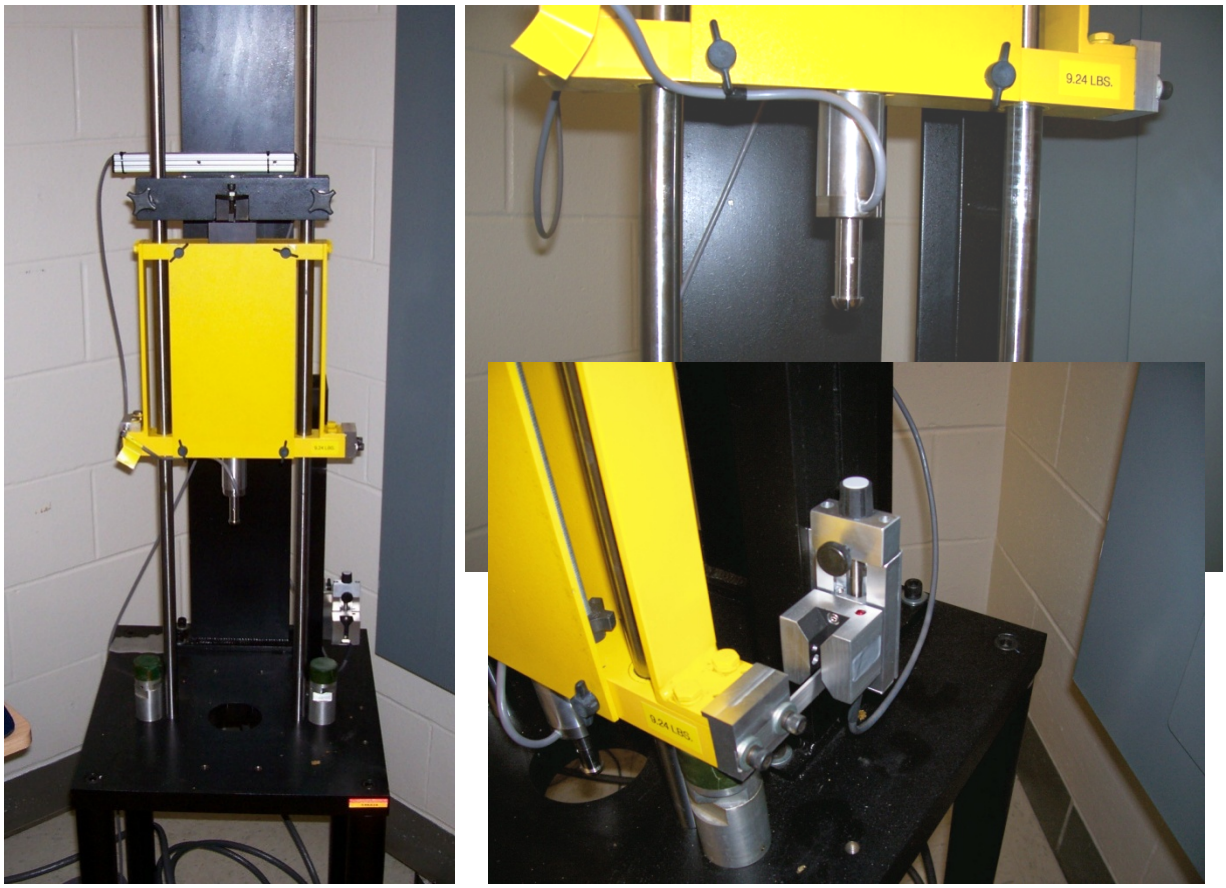

Figure 4: Instrumented Impact machine, striker, and optical velocity sensor

The vast majority of research into low-velocity impact damage of composites utilizes a drop-weight impact device with a hemispherical tup. Non-instrumented impactors can consist of a hollow cylinder inside which the impactor is dropped. Instrumented impactors (Figure 4) generally have a rail cart setup that allows for adjusting the mass and drop height. Instrumented systems require a method to measure striker velocity at the moment of impact. An instrumented tup records voltage versus time. The load cell in the tup is calibrated to convert that voltage to a given force. Since the force (F) is recorded versus time and the mass is known, the acceleration can be calculated using the expression

,

where *M* is the mass of the impactor; *a(t)* is the acceleration with time. The impactor velocity with time is calculated by

$$V(t) = V0 - \int a(t)\mathrm{d}t,$$

where V_0 is the measured impact velocity. The displacement, δ, with time can be calculated by

$$\delta(t) = \int V(t)\mathrm{d}t.$$

The impact energy *E(t)* can be expressed by integrating the force/displacement curve during the interval in which the tup is contacting the panel

$$E(t) = \int F(t)\Delta(t)\mathrm{d}t$$

where $\Delta(t) = d\delta(t)/dt$ [59].

A panel which does not suffer any damage will theoretically elastically return all the impact energy back into the impactor by way of rebound and will have zero net energy transfer (negating friction). Energy that is transferred from the impactor's potential energy to the panel that is not returned through rebound is generally consumed by the damage of the sample. A sample chart of the impact response curves is shown in.Figure 5.

The impact event itself causes a combination of damage modes as illustrated in Figure 7. Through-ply matrix microcracks and fiber breakage occur in Mode I failure. Matrix microcracks generally occur in a conical region, radiating out from the point of impact. The delaminations occur in Mode II shear as the panel flexes.

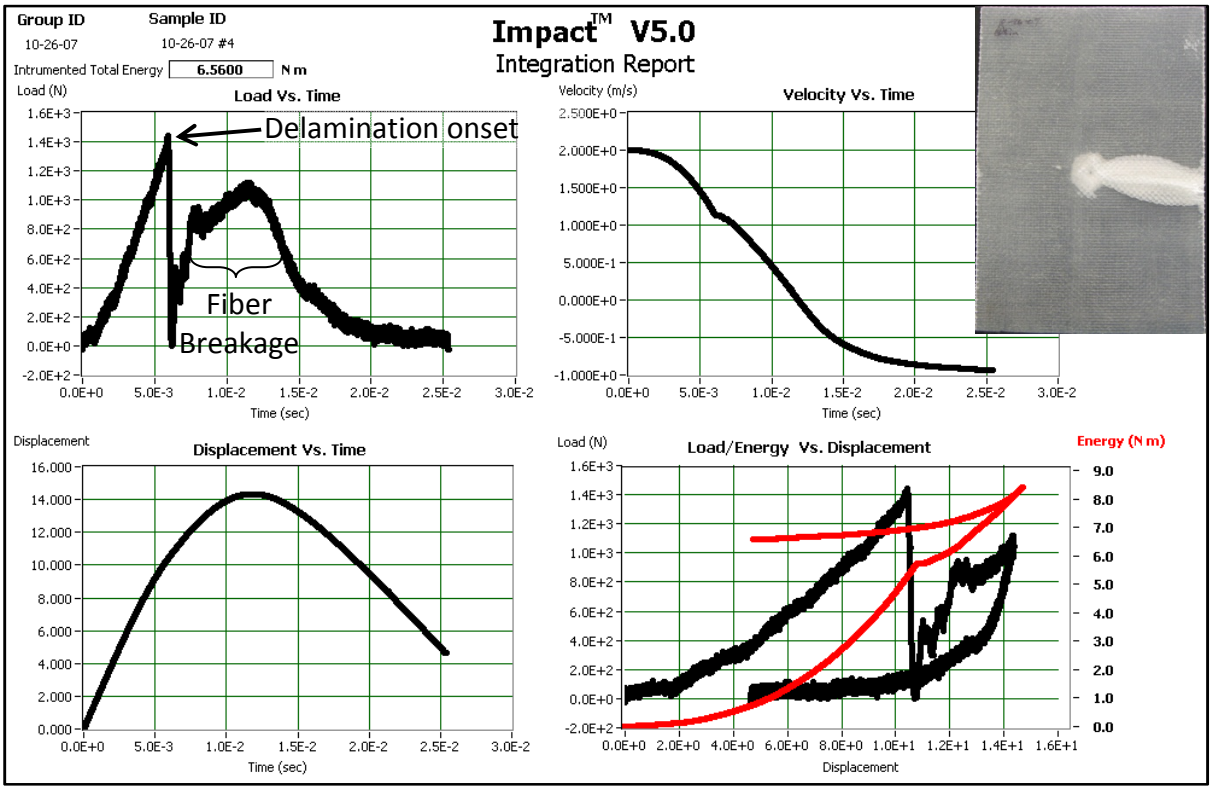

Figure 5: Impact graph, photo of sample with moderage delamination

The initial slope in the load vs. time graph (top left) is similar to a standard force/displacement curve showing the bi-axial bending of the panel. The first large drop in load is an indication that a critical threshold force for onset of delamination has been reached. From here, the sample has not failed completely, but has a reduced transverse stiffness as the load increases again. The next region represents the response to fiber breakage [59]. By contrast Figure 6 shows the graph for a panel that exhibited minimal delamination but more fiber breakage. Less than half as much energy was consumed in damaging the sample in Figure 6 as the sample in Figure 5. This variation in damage response from identical panels subjected to identical impact conditions supports the findings of an FAA study [64]

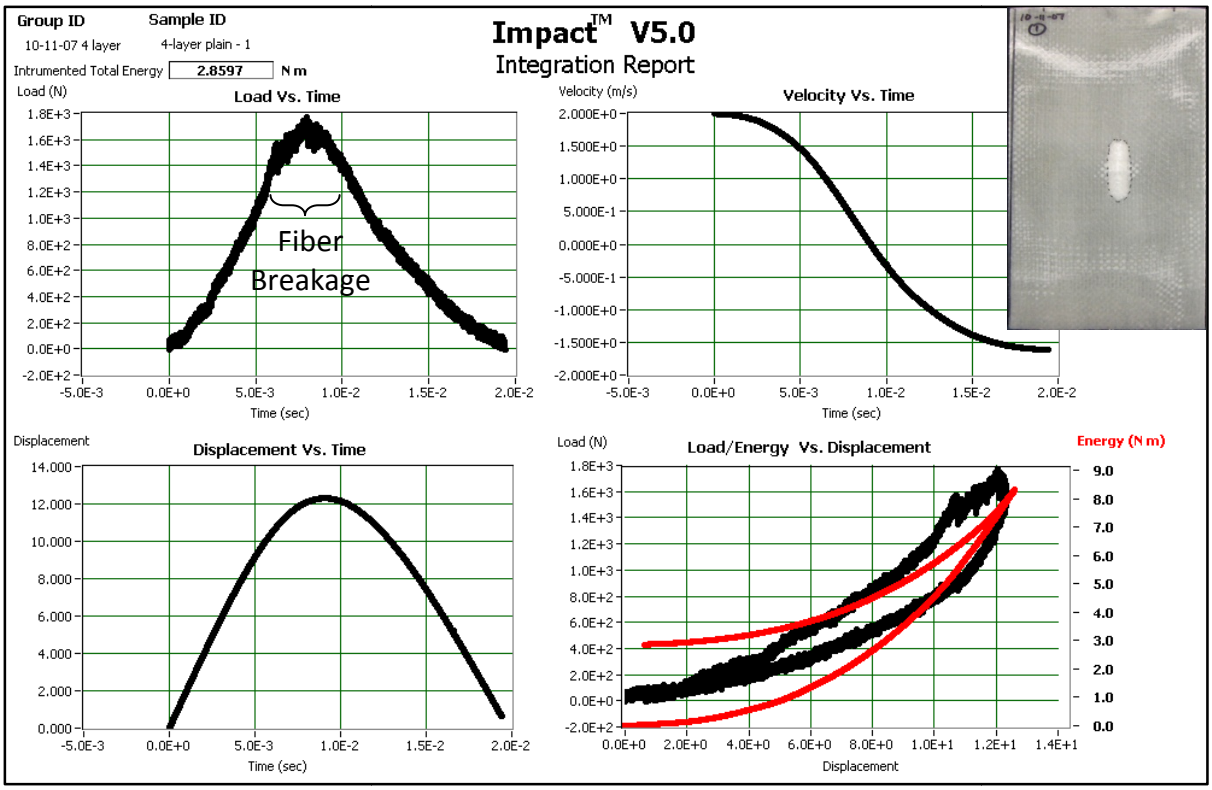

Figure 6: Impact graph, Photo of sample with minimal delamination (taken after CAI)

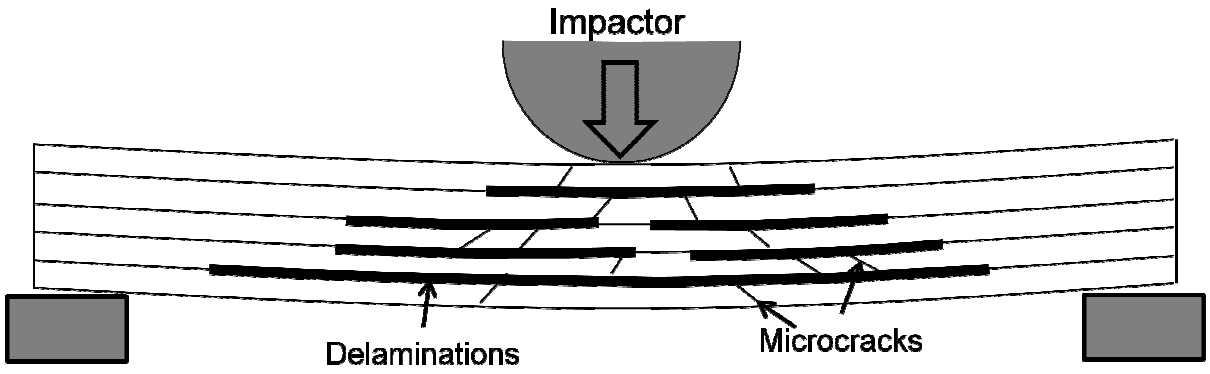

Figure 7: Schematic of impact of composite sample

The factors involved in determining the impact response of a composite panel can be divided into three categories. Some of the factors are intrinsic to the material i.e. fiber type, fiber orientation, fiber weave, matrix type, fiber volume fraction, lay-up sequence, ply

thickness, number of plies, processing conditions, matrix cure state. For example Kumar et al showed that epoxy based FRCs are the most damage tolerant if the epoxy has been post-cured at precisely the glass transition temperature of the epoxy [65]. Other extrinsic factors are related to the impacting object i.e. impactor shape, size, mass, and velocity at impact. Structural variables also play a role, namely panel geometry, support geometry, clamping conditions, the presence, nature, and spacing of stiffeners, even temperature can play a role. Many studies have investigated the influence of various of these parameters, individually and in combination.

Several studies have shown that the critical load to initiate damage is proportional to the laminate thickness raised to the 1.5 power [54], [59]. [54]'s investigation concluded that the fracture toughness of the matrix has a significant effect on the impact response, while the fiber strength and stiffness do not. The FAA conducted, commissioned, and summarized research into the relative influence of many of these factors [64]. This factorial testing compared a high and a low level for many different parameters. They determined that amongst the intrinsic material variables, the most influential for the following types of damage are:

Table 1: Most influential intrinsic parameters on damage

Rank	Parameter	
	Dent Depth	Damage Area
1	laminate thickness	matrix type
2	fiber volume ratio	fiber volume ratio
3	matrix type	fiber type

These results are consistent with Cartie's findings that since the load and damage is normal to the plane of the fibers, they will not play as big a role in impact response as matrix considerations [54].

Comparing both intrinsic and extrinsic factors yields the following indications:

Table 2: most influential parameters on damage

Rank	Parameter	
	Fiber Failure Length	Damage Area
1	impact energy	impact energy
2	impactor diameter	impactor diameter
3	laminate thickness	matrix type

In general it was seen that the extrinsic variables had a bigger influence on impact response than did the intrinsic material properties [64].

Because damaged composites have reduced abilities in compression one of the most useful methods for comparing impacted panels is in compression after impact (CAI). CAI testing is conducted with a fixture (Figure 8).that secures the top and bottom of the sample as well as the sides to prevent the sample from failing in a simple flexure or buckling mode

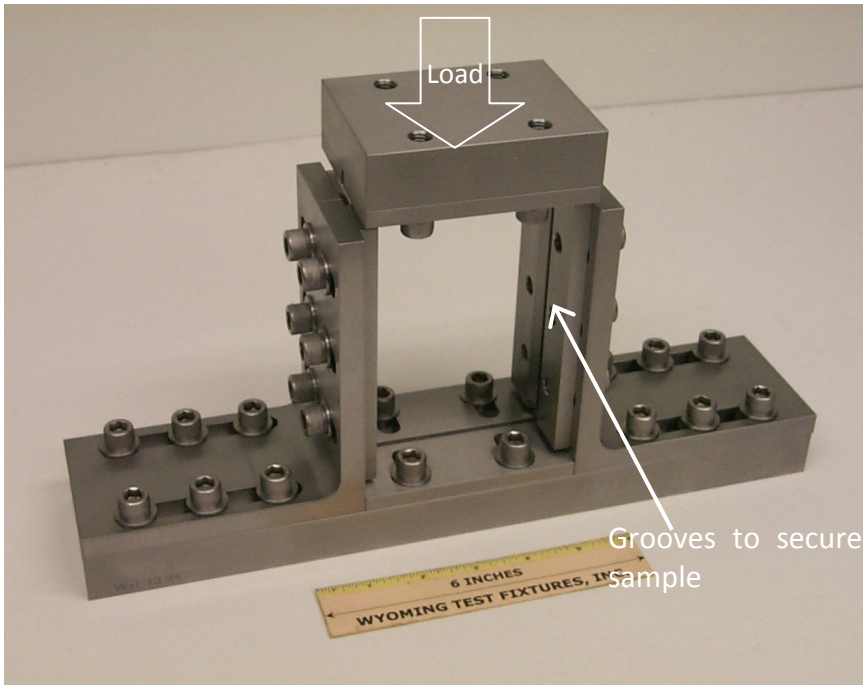

Figure 8: Compression after impact test fixture (Wyoming Test Fixtures)

Compression after impact testing typically forces a failure either by extending the delamination area out from its initial boundaries both up and out toward the panel sides, or by a buckling crack that runs through the damage area. De Freitas et al [62] found that in general panels that had suffered high impact energy tended to fail under CAI loading with all the plies moving together in the direction of impact, while lower energy impact resulted in a split with some plies buckling toward the front and some toward the back of the panel, as seen in Figure 9. In addition, the low impact energy samples typically had more displacement in the direction of impact. The direction opposite the impact for low energy was about the same as with the impact for the high energy [62].

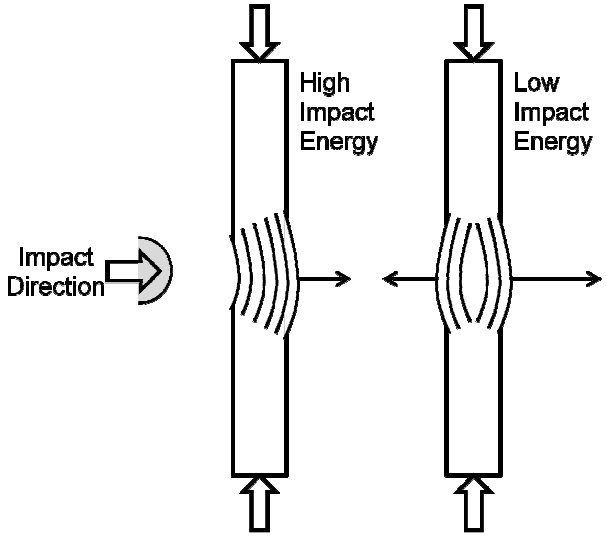

Figure 9: CAI displacement

1.4 Research objectives

1.4.1 Comparison of Healing Agent Candidates

While much work has been done to develop and fine tune the self-healing system there remains much potential for improvement. The aim of this work is to investigate the comparative healing strength of different ROMP monomers, blends, and additives as potential healing agent candidates. Some of these candidates have been selected because they require a lesser catalyst loading for polymerization, they polymerize more rapidly, or they offer the potential for increased strength or toughness.

1.4.2 Potential for Healing of Impact Damage

Several studies have experimented with the ability of a microencapsulated healing agent to adhere the crack faces of composites subjected to Mode I stress. The potential to heal the more complicated failure modes that result from impact damage of fiber-reinforced composites has not been investigated. A composite consisting of numerous plies of a polymer matrix and strengthening fibers can experience delamination between the plies, a fiber-matrix separation, fiber breakage, matrix cracking and fiber pullout. The Army Research Office provided the funds specifically to investigate healing of this mixed-mode failure.

1.4.3 Novel Method for Quantifying Damage and Healing

An advantage to the use of glass fibers as the composite reinforcement is that delaminations and cracks provide a visual contrast to the intact regions. This allows for an easy method for quantifying the damage area. The visual appearance of the damage area changes upon contact with the healing agent, but it is not possible to assess visually whether the two faces have simply been wetted and released or if there is a solid bond between the crack planes. Ultrasonic c-scan was used to map the initial impact damage, and then repeated after the healing event to generally assess the effectiveness of the healing agent at filling the crack volume and bonding to all crack faces. While ultrasonic C-scan has been used by many researchers [62], [54], it has not previously been used to assess the effectiveness of a self-healing repair agent.

CHAPTER 2 COMPARISON OF HEALING AGENT CANDIDATES

2.1 Abstract

The fundamentals of self-healing through an embedded microencapsulated healing agent have been developed and have demonstrated an impressive degree of healing efficiency. The aim of this project was to investigate potential improvements to the system. Specifically, several other monomers , blends, and additives exist that could potentially give better properties to the healed system including: faster cure time, better crack area coverage, decreased catalyst usage, stronger loads at break, increased elongation at break, increased energy to failure, increased temperature capabilities, increased chemical compatibility, increased shelf-life. This investigation looked specifically at comparing the Mode I fracture strength of the different healing agent candidates.

2.2 Introduction

While the ROMP reaction produces good quality polymers there are some drawbacks to the current system. The reaction requires that the monomer come in contact with, and dissolve, the catalyst. Grubbs' catalyst is prohibitively expensive for wide use in large-scale applications. The more the catalyst quantity can be reduced without suffering dramatic decreases in properties the more cost-efficient and practical for real world applications. In addition, the epoxy hardener reacts with the catalyst decreasing its efficiency, necessitating a protective mechanism. Rule, et al, demonstrated the effectiveness of encapsulating the catalyst in wax and imbedding the wax-protected catalyst

along with the microcapsules. While there was some concern that the presence of microcapsules would decrease the virgin properties of the composite, Brown *et al.* showed that the fracture toughness increases with the inclusion of microcapsules [40]-[41]. No such improvement accompanies the inclusion of wax microspheres. Not only is less of the expensive catalyst needed, less wax in the composite results in a lessened decrease in strength.

In addition to different monomers, the effect of addition of various cross-linking agents and nanotubes was proposed. The in-house synthesized cross-linkers should provide additional cohesive strength to the healing agent.

It was hypothesized that the ENB, exo-DCPD, and nanotube systems would polymerize faster than DCPD at equivalent catalyst levels and it would need to be investigated whether their strengths were comparable. If so, would it be possible to decrease the catalyst amount and still get favorable properties?

2.2.1 Healing Agent Factors

A number of variables with the healing agent affect the healing performance. The cure time and temperature have a strong effect on mechanical properties. Different healing agent monomers have a host of different properties. An ideal monomer should have good mechanical properties – high adhesive and cohesive strength and fracture toughness. It should have good reaction kinetics – rapid polymerization and cure yet not so rapid as to envelop the catalyst in a protective layer before the catalyst can completely dissolve, which

would leave areas unpolymerized. The monomer must have low viscosity so it can flow into extremely narrow microcracks as well as good surface interaction with the matrix [24].

The first system to successfully demonstrate healing used dicyclopentadiene (DCPD) for the healing agent monomer and Bis(tricyclohexylphosphine)benzylidine ruthenium (IV) dichloride (Grubbs' catalyst) as the catalyst/trigger [14]. This combination is one of many potential ring-opening metathesis polymerization (ROMP) systems that can potentially be used for self-healing applications. As the first successful system virtually all modifications are compared to the effectiveness of the initial work. The chemical mechanism proceeds thus:

> "First, the ruthenium metal carbine and the cycloalkene combine to form an intermediate metallacyclobutane. The metallacycle then breaks between the atoms that initially shared a double bond and the new olefin that is generated remains attached to the catalyst as part of a growing polymer chain. The driving force for the reaction is the relief of ring strain." [14]

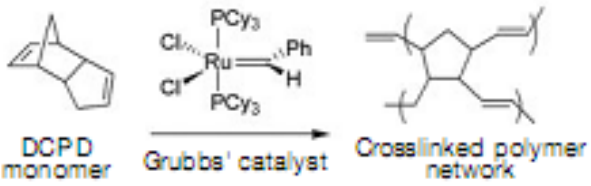

Figure 10: DCPD reacts with Grubbs' catalyst resulting in a crosslinked polymer network

Some ROMP monomers, including DCPD, have a second cyclic double bond that can act as an excellent site for further polymerization into a crosslinked network [35]. DCPD is

commercially available, inexpensive, has acceptable room-temperature viscosity, and polymerizes at room temperature with Grubbs' catalyst. There are several manufacturers of endo-DCPD and different purity levels are available commercially. Above approximately 95% purity the endo-DCPD solidifies at room temperature, which is unacceptable as a healing agent candidate. The ROMP behavior of DCPD was described thermally by Kessler *et al*. through the use of differential scanning calorimetry, first for endo-DCPD [28], and then for exo-DCPD [29]. While the exo- configuration is not commercially available, it is synthesized from commercial endo-DCPD as detailed in [31]-[48]. Exo-DCPD was found to be much more reactive than the endo- configuration and required significantly less catalyst to polymerize, and polymerized much faster [29]-[30]. Each of these differences appears to provide significant advantage over the endo- configuration. Endo-DCPD takes just beyond 10 hours to approach full healing efficiency at a catalyst concentration of 2.0 mg/cc. By contrast exo-DCPD polymerizes 20 times more rapidly, developing mechanical properties in a matter of minutes. Slight increases in healing efficiency continue until a little less than 5 hours. The reduction in time coincides also includes a reduction in healing efficiency, from approximately 60 to 40 % [47]. Mauldin et al also investigated endo-exo- blends and found that healing efficiency increases with the % of endo- up to a maximum value of ~60%, the same efficiency that endo-DCPD itself had [47].

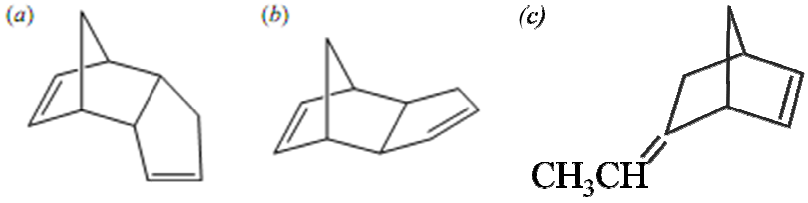

Figure 11: Chemical structure of (a) endo-DCPD, (B) Exo-DCPD, and (C) ENB

Another ROMP monomer that has been investigated is 5-ethylidene-2-norbornene (ENB). ENB has the potential to be an improvement over endo-DCPD: it polymerizes much faster and requires an order of magnitude less catalyst. It does not form crosslinks to other chains as readily as does DCPD. Lee *et al.* characterized ENB for comparison to endo-DCPD as well as comparing blends of the two [49][50].

The rapid polymerization of ENB and exo-DCPD runs the risk of being too rapid. Two potential problems present themselves with too-rapid polymerization. The first is that the liquid healing agent could begin to polymerize and harden before it has reached the full extent of the crack. The second scenario is if the polymerization rate is much faster than the catalyst dissolution rate the system could form a polymer barrier sealing off the local region immediately surrounding the catalyst. This leaves adjacent regions unpolymerized. [47]

A host of additives can influence the healing ability of any monomer. Crosslinkers may be added to provide added strength and stiffness [25]. Nano-scale additions such as fumed silica and carbon nanotubes can have an impact as well. Different additives can influence the processing, transport, release (wax dissolution kinetics), and polymerization characteristics (i.e. T_g, rate of reaction). As mentioned previously, different monomers,

blends, crosslinking agents, and nano-scale additives will all alter the processing specifics and may make it difficult to create microspheres of comparable diameter, thickness, strength, and durability. These changes make it difficult to make an apples-to-apples comparison of healing abilities.

2.2.2 Catalyst

There are many advantages to systems which do not require as heavy catalyst loadings. All forms of Grubbs' catalyst have a high cost, which drives research toward more cost-effective solutions: higher reactivity monomers, higher reactivity catalysts, more effective catalyst morphologies, better distribution of catalyst, and substitution of less-expensive catalysts. Lower loadings mean significantly lower cost for the composite as a whole, which increases the potential for commercial use. Second, while the wax does protect the catalyst from degradation by the epoxy curing agent, it does not add any strength to the system. The wax is significantly softer than the epoxy matrix and also acts as a plasticizer, softening the healing agent it is dissolved in. Less catalyst means less wax altogether.

There are several suppliers of 1st Generation Grubbs' catalyst, who each provide crystals with different morphologies. Typically the as-received catalyst comes as crystals that are too large, which uses the catalyst inefficiently. Smaller crystals are more readily dissolved in the monomer. Further, a greater number of smaller catalyst crystals decreases the potential for the aforementioned scenario in which polymerization occurs faster than dissolution can distribute the catalyst. Different catalyst recrystallization strategies (freeze-

dry vs. dissolution in methylene chloride and evaporation of solvent) result in different catalyst morphologies which result in different dissolution rates and, thereby, polymerization times, all superior to as-received [34]. Reducing the catalyst particle size through mechanical ball-milling produces the same effect [31]. Some studies have shown that 1st Generation Grubbs' catalyst has limited temperature stability – losing effectiveness at temperatures above approximately 90°C. While the true self-healing system should occur without requiring external heat, many polymer matrix systems require heat for the initial cure and frequently for a post-cure step to achieve optimum properties.

Another approach is to seek out a catalyst that is less reactive with the DETA. 2nd Generation Grubbs' catalyst and Hoyveda Grubbs catalyst are similar catalysts that may have higher reactivity and stability, but higher cost per weight. Wilson et al [53] investigated the effectiveness of various ruthenium-based catalysts for ROMP applications. A less expensive catalyst option is WCl_6, but even at much greater loading strength is still reduced. WCl_6 still suffers from many of the same reactivity reducers as Grubbs' catalyst [52]. A different approach from Grela and Kim produced a much cheaper ruthenium-based catalyst from α-asarone that is somewhat less effective [51]. Likewise, a different curing agent such as an anhydride, could be used in the matrix that would less adversely affect the catalyst [38].

Another concern is that 1st Generation Grubbs' catalyst has limited temperature stability and most epoxy systems require external heating to fully [53].

2.2.3 Other polymerization factors

Aside from the physical and chemical structure of the healing agent and catalyst, a few other factors influence rebonding ability. Probably the biggest other factor in polymerization properties is the concentration of the reactants. Higher catalyst loadings help the reaction occur more rapidly and proceed more fully, resulting in better mechanical properties. The potential healing benefits of increased microcapsule and catalyst loadings must be weighed very carefully with the effect on properties of the bulk composite. It does not serve to increase the healing efficiency as compared to the bulk properties by diminishing the bulk properties. An early concern with such a system was that the inclusions would decrease the initial strength of the system. It was shown by Brown *et al.* that while the maximum load the system was able to support did decrease slightly with the inclusion of microcapsules, the fracture toughness increased by 27% on average [40][41]. As with virtually any polymerization reaction, the cure conditions affect final properties. Additional heat and time are likely to help any system react more fully.

2.3 Experimental

The first goal, comparing healing agent candidates, consisted of two different tapered double cantilever beam configurations. Width-tapered double cantilever beams (WTDCB) were used to compare adhesive capability of the catalyzed healing agents to epoxy surfaces. Height-tapered DCB specimens were used to more closely approximate self-healing conditions. Three phases of HTDCB testing occurred. The first phase consisted of applying catalyzed healing agent to the central crack plane. Phase two consisted of embedding wax-

protected catalyst into the area surrounding the likely crack plane, and applying uncatalyzed healing agent to the crack plane. This phase is referred to as self-activating. Finally, the self-healing phase consists of embedding both microencapsulated healing agent and protected catalyst into the area surrounding the likely crack plane.

Procedures

WTDCB specimens

The steel parts to the WTDCB specimens were machined out of 0.125 in. thick steel plate. End tabs with 0.25 in. diameter pinholes were welded onto the ends. The flat face was first roughened with 60 grit sandpaper to improve adhesion between the epoxy layer and the steel and ensure that failure occurred between the epoxy faces, either adhesively or cohesively. After roughening the steel pieces were rinsed in water and placed in an ultrasonic water bath for five minutes to remove potential debris and loose material caused by the roughening process. After ultrasonication the samples were rinsed with water and then with acetone to remove any potential fingerprints or grease-like contamination that would adversely affect the steel/epoxy interface, and dried with forced air.

The cleaned steel pieces were positioned face up with a layer of tape (3M Colored Plastic Tape – Clear, ¾") around the perimeter with 0.125-0.25 in. standing vertically above the steel face. This produces a mold for hold the epoxy. The epoxy (~45g to make 10 pieces) was mixed per the normal method – 10:1 Epon 828 epoxy: EpiCure 3223 hardener and was poured into the mold. The samples were allowed to cure at room temperature for 24 hours. Elevated temperatures cure the epoxy quicker but frequently resulted in the epoxy separating from the steel during pull testing – most likely due to the thermal

expansion mismatch. After the one day cure the tape was removed. The epoxy level varied due to the meniscus effect and the variable width of the sample causing varying curvature. The narrow end resulted in a positive meniscus with excess material above the tape level while and the wide end had a negative meniscus with the epoxy level below the tape. These uneven samples were evened out by hand grinding the epoxy flat on a metallographic grinding wheel with 200-grit, 8-in diameter paper. Once the epoxy layer was level and to a thickness of 0.1 in the samples were again placed in the ultrasonic cleaner to remove loose material and rinsed with water and acetone to produce a clean surface.

Cleaned samples were arranged face up, with a support under the wide end to keep the samples level. The healing agent candidate and catalyst were mixed by hand in a vial until the catalyst had visibly dissolved. The catalyzed healing agent was then applied generously by syringe to the epoxy surface. A matching top piece was placed on top, starting at the narrow end to avoid trapping bubbles in the healing agent. The two halves were clamped together with 1.5 in. binder clips. During this process the excess healing agent flowed easily over the edges. Those parts that were not blocked by the binder clips were wiped clean to prevent polymer from binding the pieces together outside of the flat surfaces. The polymer shielded by the clamps was easily removed after removal of the clamps. The samples were allowed to cure for 24 hours at room temperature before testing. Prior to testing the edges were painted with white correction fluid to aid in observing the crack tip progression.

The healing agent candidates have been tested by means of a width-tapered double cantilever beam (WTDCB) specimen. Steel WTDCB specimens were coated with an epoxy

layer then glued together using the various monomer-plus-catalyst systems and allowed to dry at room temperature. The candidates tested have been endo-DCPD, exo-DCPD, ENB, ENB with 4 wt% Cross Linker 2, and a 3:1 ENB:endo-DCPD mixture. The samples were then pulled apart in Mode I failure using a tensile test machine seen in Figure 12.

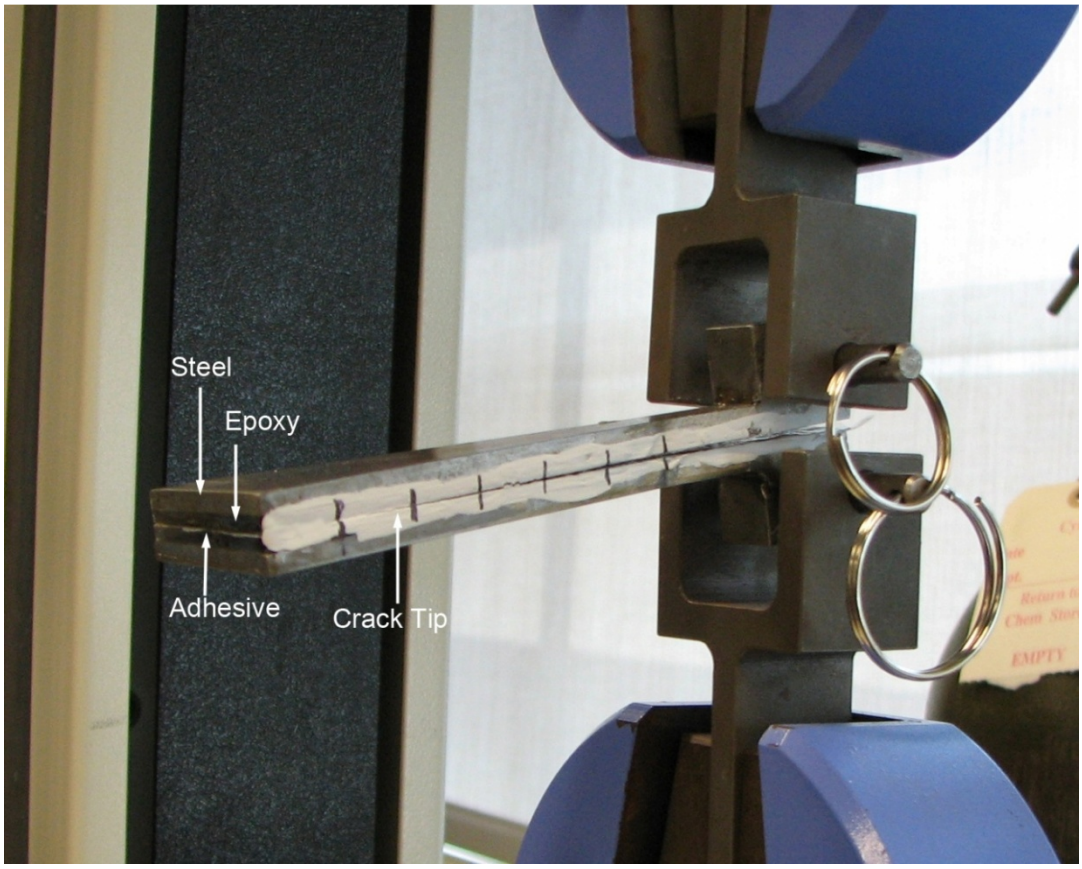

Figure 12: WTDCB specimen in test fixture

2.4 Results and Discussion

2.4.1 WTDCBs

Data for each sample has been collected and compared with regard to Maximum Load, Area under the Load/Stroke curve, and Stroke at Failure. Results are summarized in

Table 3 and Figure 13: WTDCB load vs. Displacement for different healing agents A significant finding is that endo-DCPD, the default monomer used in the groundbreaking work, has shown the poorest results in nearly every category, indicating considerable potential for mechanical improvement based on changing the healing agent. Exo-DCPD showed approximately a 20% increase in maximum load, 8% increase in total energy at failure, and 13% decrease in stroke at failure over endo-DCPD, at only half the catalyst loading. ENB, which polymerizes at a tenth of the catalyst loading of endo-DCPD showed nearly a two-fold increase in maximum load, a 140% increase in energy at failure, and a 25% increase in stroke at failure. The addition of 4 wt% Cross Linker 2 to ENB decreased the maximum load by 10%, decreased the energy at failure by 18% and the stroke at failure by 6%. It was expected that the addition of the cross linking agent would make the adhesive more brittle and perhaps less able to absorb the same total energy in deformation prior to failure. It is also worth noting that a significant amount of scatter has been present within each configuration, so the decreases manifest in the ENB with cross linking agent very well might be accounted for in the scatter. The ENB (3): endo-DCPD (1) mixture has shown a significant improvement over the other monomers. This mixture exhibits a 140% increase in maximum load over endo-DCPD, 18% over pure ENB; a four-fold increase in energy at failure over DCPD, 30% over ENB; and a 70% increase in stroke at failure over DCPD, 21% over ENB.

Table 3: WTDCB Average values

Healing Agent, catalyst loading	Max load (kN)	Area under curve (Nm)	Stroke at Failure (mm)
Endo-DCPD 2.0 mg/mL	0.04420	0.09910	2.96560
Exo-DCPD 0.2 mg/mL	0.05353	0.10705	2.57690
ENB 0.2 mg/mL	0.08150	0.23693	3.68480
ENB + 4% CL2 2.0 mg/mL	0.07336	0.19483	3.46185
E3D1 0.5 mg/mL	0.10506	0.39842	5.01030

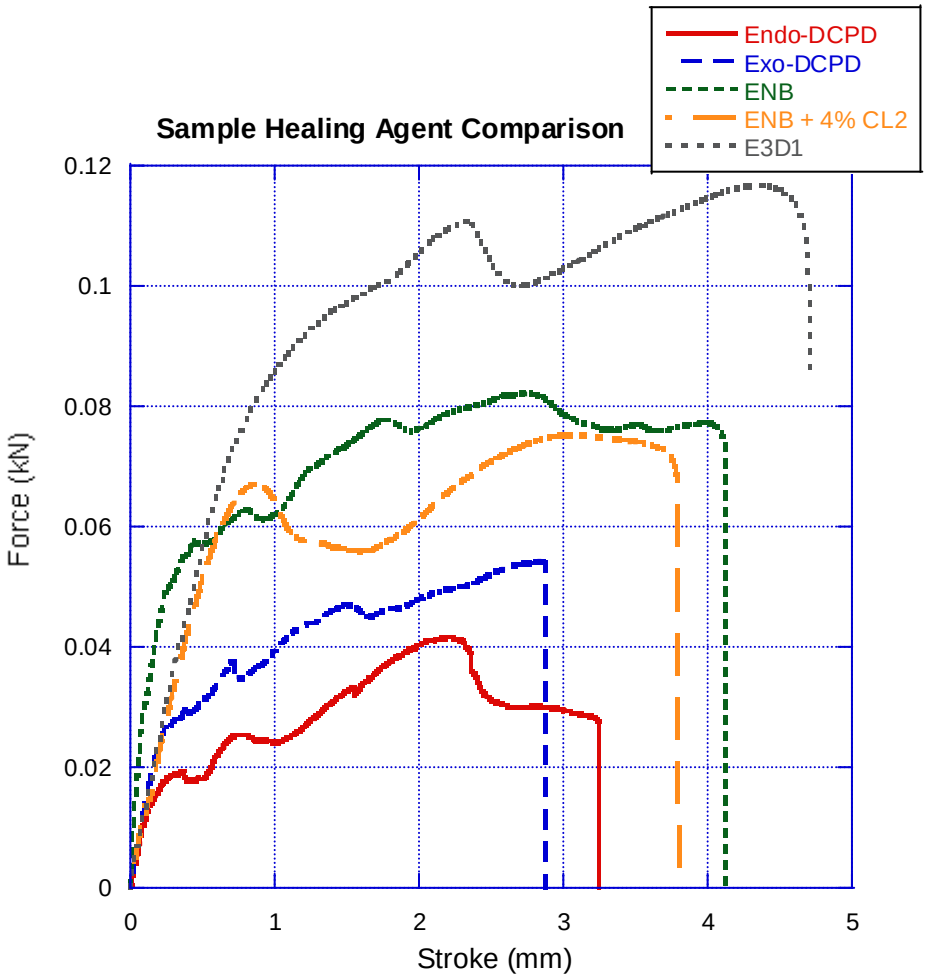

Figure 13: WTDCB load vs. Displacement for different healing agents

While the WTDCB tests gave strong preference to the use of ENB as the healing agent, that test method had some limitations. The load frame available at the time of testing was unable to ensure proper alignment of the specimens to ensure purely Mode I failure. The weight of the specimen caused a rotation about the lower grip, resulting in the samples being tilted downward approximately 10-15° from horizontal. This arrangement puts the samples under some degree of Mode II shear that the load frame cannot distinguish from Mode I. Even so, the ENB shows a significant advantage over either DCPD isomer.

The original plan was to test the healing agent candidates under three different conditions: 1) inject catalyzed monomer onto the plane; 2) embed the catalyst in the epoxy, expose the catalyst, and inject monomer onto the plane with the exposed catalyst (self-activated system); 3) embed both catalyst and microcapsules in the epoxy (self-healing system). While the WTDCB system was good for method 1, no system could be devised to reliably and consistently expose the catalyst or open the microcapsules. It was determined to shift efforts to a Height Tapered double cantilever beam (HTDCB) system. Mauldin et al. released results comparing endo- and exo-DCPD for HTDCB specimens, so that variable was dropped from the HTDCB testing.

2.4.2 HTDCBs

Height-tapered DCB specimens began with an aluminum master mold. The aluminum mold was used to create molds from silicone rubber (Silastic J, Dow Corning). The rubber molds were produced by mixing the Silastic J base with the catalyst 10:1 by

weight and mixed by hand. This mixture was placed in a vacuum chamber until the bubbles had expanded and then collapsed (~30 minutes). It was then poured into the aluminum mold and placed in the vacuum chamber again to remove bubbles from the corner and edge locations where they tended to remain after pouring. After this second vacuum cycle the molds were allowed to cure for 24 hours at room temperature, after which they were removed.

For neat epoxy samples five to seven sets of molds were prepared and separated with a 0.125 in. coupon of high impact polystyrene (McMaster-Carr) in between each mold pair to better distribute the load and prevent adhesion between the different mold pairs. The entire set of molds was compressed slightly by two adjustable Irwin Quick-Grip Clamps at the top and bottom. The clamps were adjusted to a compressive force that could still pivot but just barely. Less force resulted in leakage from the molds and slightly thicker specimens overall. More force tended to compress the notch regions together. This resulted in specimens with significantly reduced width in the desired crack plane, rendering the samples useless. The epoxy was mixed by hand per the manufacturer's instructions at 10:1 resin to hardener by weight. Before pouring the mixture was placed under vacuum until the bubbles had risen and collapsed (~25 minutes). The degassed epoxy was then poured into the molds and allowed to cure at room temperature for 24 hours. After this cure the epoxy HTDCB samples were removed from the molds. If epoxy was present connecting the top edges it was removed carefully with a jeweler's saw.

The final task before pulling in the Instron was creating the precrack. A small groove (~1-2 mm) was placed at the beginning of the notch area with the jeweler's saw to provide a

more consistent location and direction for the razor blade. The razor blade was inserted into the groove and the sample was turned so that it was supported entirely on the razor blade, which was in turn supported by aluminum supports. The wide end of the sample was tapped gently with a hammer or mallet until a short precrack formed. At this point the sample was ready for testing.

For self-activated (Phase II) and self-healing systems (Phase III) a separate silicone rubber spacer was placed in the center of the mold. This produces samples that possess the potential for self-activated healing or self-healing, but do not waste the self-healing materials in regions of the sample where the crack should not pass. Given the high monetary and labor cost of the self-healing materials any system which retains the necessary self-healing functionality while reducing the total consumption of such materials is a stride toward commercial viability. Epoxy for the sides was mixed as stated above. This was poured in over the spacer and into both sides of each mold pair and allowed to cure as above. After cure the molds were opened and the center spacer was removed. More epoxy was prepared as before, after which the wax-protected catalyst, microcapsules, and Cab-o-sil were stirred in gently to avoid creating additional bubbles. This mixture was much thicker and was poured into a much smaller opening due to the epoxy side pieces blocking more than half of the opening. It was much more common for the epoxy to cover the opening completely which impedes flow considerably. When this happened a thin wooden stick was used to reopen the air path to the bulk cavity which would restore flow. This system underwent the same cure schedule as the neat epoxy. An alternate method involved removing the center piece while leaving the two epoxy sides in place with the mold

open and lying flat. The normal opening was covered with tape to act as a dam and the cavity was filled with only half of the mold in place. After filling the cavity the top half of the mold was placed. Multiple molds were prepared this way and stacked on top of each other. After 30 minutes the stack was flipped over as an additional precaution in case the materials were to segregate. This method proved much easier and quicker but did result in excess mixture spilling onto the flat faces of the neat sides. When molds from this second style operation were opened yellow regions were present among the excess epoxy on the neat sides indicating some capsules had been ruptured by the mold and had encountered catalyst and polymerized.

The HTDCB sample equations assume a sharp crack is already present. A precrack was tapped in with a razor blade after which the two halves were strained in tension until the sample broke down the middle. The results for the samples with precracks are shown in Figure 14 and Table 4 .

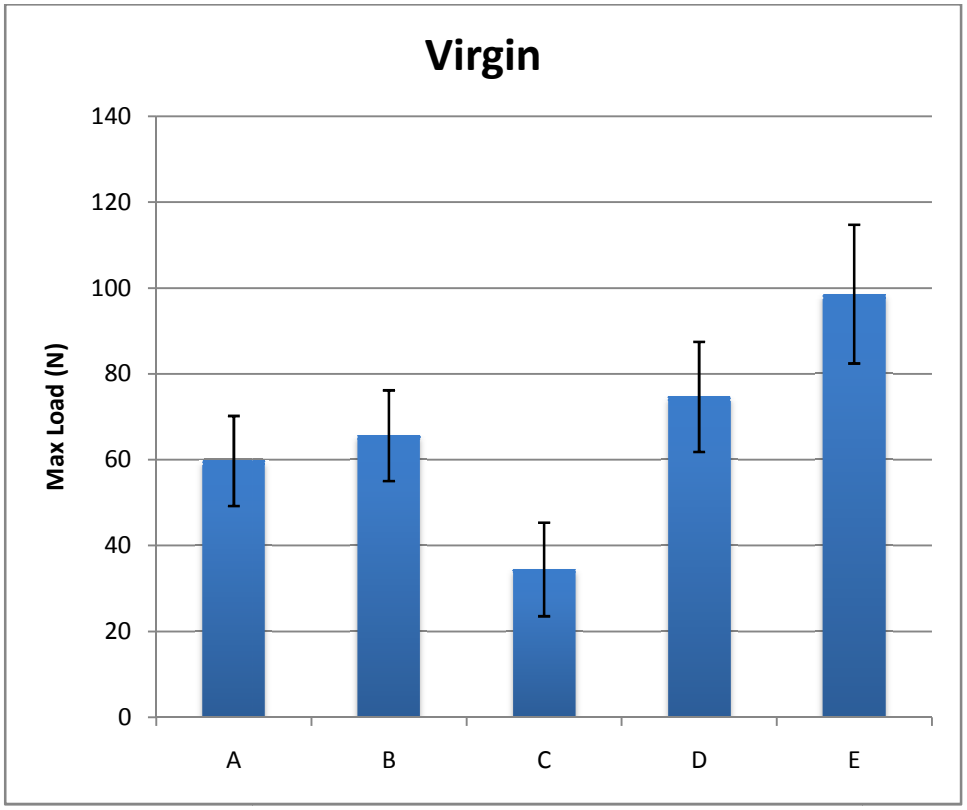

Figure 14: HTDCB original max loads

Table 4: HTDCB Specimen details and results

Sample	**A** (Neat epoxy)	**B**	**C**	**D**	**E**
Cab-o-sil %	N/A	1.0	1.0	1.0	1.0
Wax Catalyst %	N/A	N/A	5.0	5.0	10.0
ENB Microcapsule %	N/A	N/A	N/A	10.0	10.0
Max Load (N)	59.73	65.62	34.46	74.64	98.59
Standard Deviation	10.48	10.57	10.88	12.80	16.14

Because a small amount of Cab-o-sil was needed to prevent the wax-coated catalyst from floating to the top of the epoxy, a batch of specimens was prepared to assess the influence of the fumed silica. Virgin maximum loads for the neat epoxy and the epoxy with added silica were very similar, within the scatter of the data. Some studies have shown that fumed silica in epoxy decreases the capacity of the epoxy until a very high loading (~30%) at

which point it increases the capacity [42]. The addition of 5 wt% wax-coated catalyst dropped the maximum loads by half. As seen in early work, the presence of microcapsules improved virgin performance. 10 wt% ENB microcapsules with 5 wt% wax catalyst increased the max load by approximately 25%. Those same conditions but with double the loading of wax catalyst cause a 40% increase over neat epoxy.

Phase I

For Phase I a catalyzed monomer was applied to the crack face and the two halved brought together again. To prevent the monomer from undergoing too-rapid polymerization prior to application the healing agent was cooled to slow the polymerization kinetics. Both the healing agent and recrystallized catalyst were kept in vials submerged in a 1: 1 water: ethanol mixture cooled with dry ice. The constituents were mixed and maintained in the bath until application on the crack plane. The sides were clamped in such a way as to prevent Mode III shear, but no additional force was applied to close the crack sides beyond the manual force that was released once the clamps were in place. The samples were allowed to cure at room temperature and then pulled apart again. The results are shown in Figure 15 and Table 5

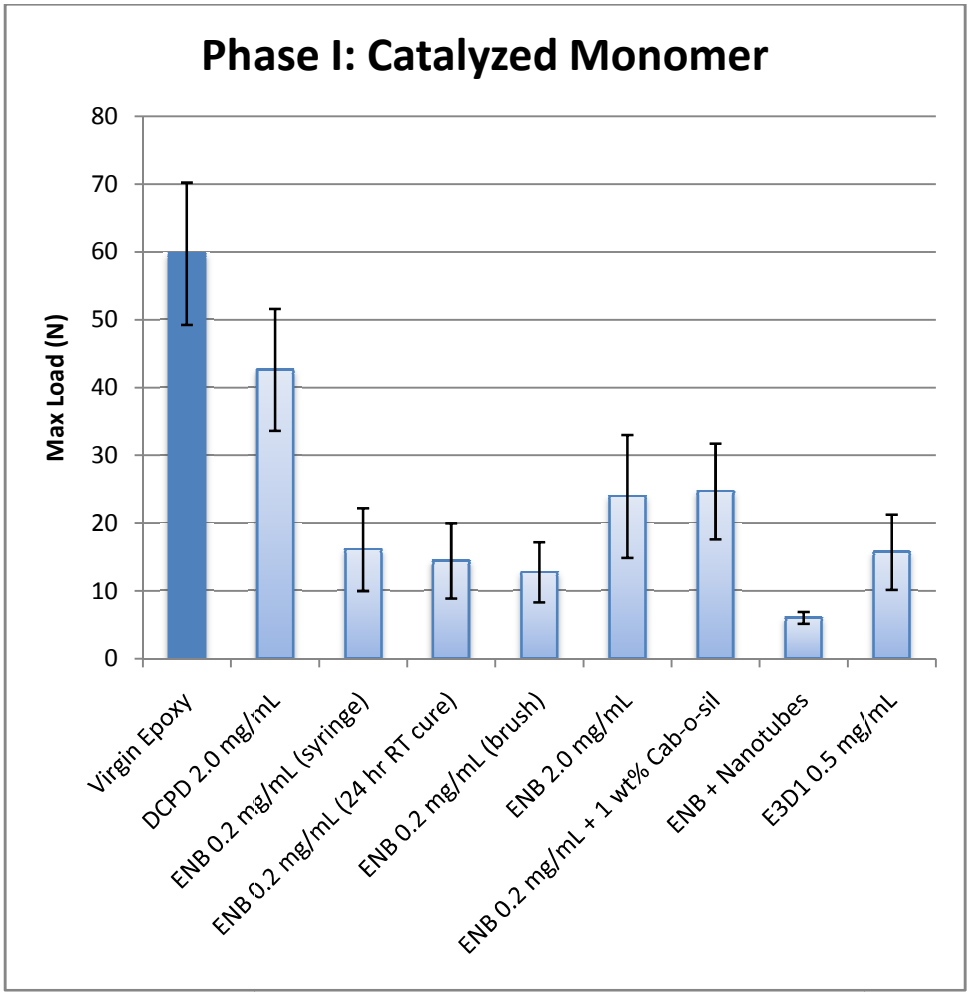

Figure 15: Phase I - Injected Catalyzed Monomer

Table 5: Phase I Results Comparison

Healing Agent	Virgin Epoxy	DCPD	ENB (syringe)	ENB 24-hr cure	ENB (brush)	ENB	ENB + Cab-o-sil	ENB + Nanotubes	E3D1
Catalyst Loading	N/A	2.0 mg/mL	0.2 mg/mL	0.2 mg/mL (	0.2 mg/mL	2.0 mg/mL	0.2 mg/mL	0.2 mg/mL	0.5 mg/mL
Max Load (N)	59.73	42.62	16.11	14.46	12.78	23.96	24.69	6.051	15.73
Std Dev	10.48	8.98	6.10	5.54	4.43	9.05	7.06	0.87	5.54
η	N/A	0.713	0.269	0.242	0.214	0.401	0.413	0.101	0.263

At the beginning of HTDCB testing the assumption was that the ENB samples would show an improvement over DCPD similar to the WTDCB samples. Surprisingly the phase I values (most similar in theory to the WTDCB) have not shown that preference (Figure 15,

Table 5). DCPD has had 2.5-3 times the maximum load of ENB. The DCPD values are 70-80% of the epoxy's virgin strength, while the ENB is 25-30%. Possible causes might be the application method, incomplete polymerization (perhaps related to the very small quantity), or the viscosity.

Initially the catalyzed healing agent was deposited on the crack face by means of a syringe. This frequently resulted in much of the liquid spilling down the sides. Sufficient liquid was always provided to bridge the crack and the excess was wiped off. Many of the ENB samples prepared this way failed to adhere the two sides together adequately to allow testing. The 'ENB 0.2 syringe' sample batch is the average of only three that survived to be tested out of approx. 12 prepared samples. A different application method – brushing – still appeared to adequately fill the crack volume with much less spillage and less material needing to be wicked out. The brush method resulted in 9 out of 12 being testable, but they did average a slightly lower failure load than did the syringe applied samples. The numbers reported do not include any values for the untestable specimens i.e. they are treated as a 'no test' and not as a value of zero. Given comparable loads reached and a better sample yield brushing was chosen as the application method for all samples excepting those mentioned as being injected.

To investigate the possibility that the reaction was not proceeding fully the catalyst loading was increased ten-fold, to the same level as the DCPD. Increasing the catalyst level

to the DCPD concentration increased the max load and healing efficiency by about double over the brush-applied ENB. Standard procedure was to allow the samples to cure for 24 hours at room temperature followed by a 24-hour post cure at 30°C. One batch of samples was made and tested after only the 24-hour ambient cure. These samples showed slightly lower maximum load values than the post-cured (14.46 vs. 16.11), but within the scatter.

The viscosity of ENB was below the range detectable by the available viscometer. Furthermore no amount of added CL-2 has raised the viscosity sufficiently to get a proper measurement of any sort. To gauge a general sense of how the behavior might change with increased viscosity a batch was prepared of ENB with 10 mg/cc of Cab-o-sil (1.1 wt%). This gave a slightly higher average load than did increasing the catalyst 10-fold. A low viscosity is a good characteristic for a healing agent as it allows the monomer to flow into all the small microcracks.

A blend of ENB:DCPD at a 3:1 ratio, with 0.5 mg Grubbs catalyst/cc of monomer gave very comparable results to plain ENB. When these sample pulled apart there was a noticeable odor matching that of the uncured monomer. These samples had a slightly higher average healing efficiency, but within the scatter of the data.

One attempt has been made to incorporate carbon nanotubes into ENB, but as the treatment process for the nanotubes to disperse in ENB has not been optimized yet, it was visually very poor dispersion. As such the clumps of nanotubes acted more as flaws than reinforcements. Only three (of eight) samples could bear their own weight and those that did had less than half of the max load of any other condition. The numbers reported treat those others as a ‘no test’ scenario and not a value of zero.

Phase II

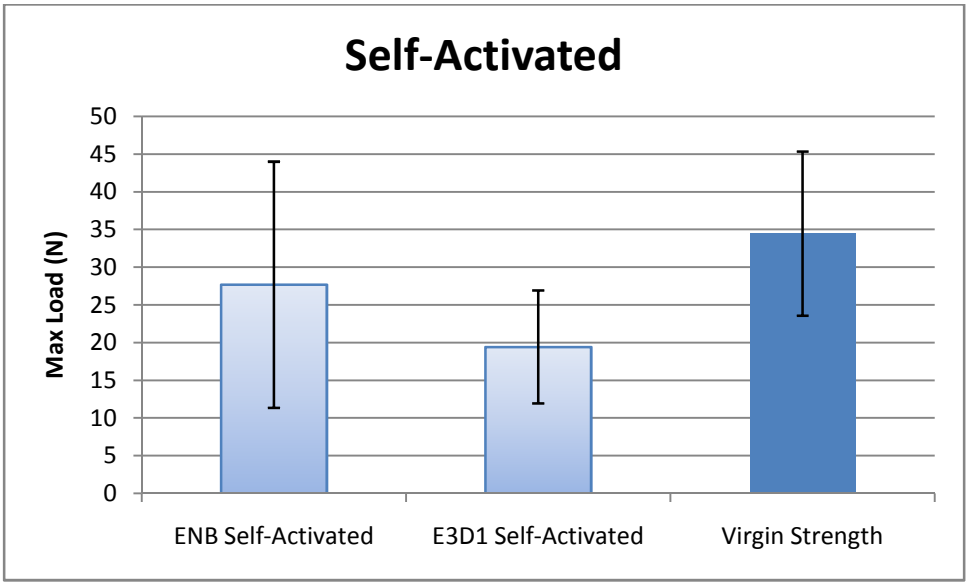

Figure 16: Self-Activated HTDCB Specimens

Table 6: phase II results comparison

Sample	Virgin Strength 5 wt % Wax Catalyst	ENB Self-Activated	E3D1 Self-Activated
Max Load (N)	34.46468	27.68792	19.43776
Standard Deviation	10.88613	16.31846	7.486639
η	N/A	0.803371	0.563991

The self-activated system (with ENB) has produced promising, if somewhat varied results. Half the samples (the bad half) had maximum strengths quite comparable to the catalyzed ENB. The other half had values three to four times as high – very similar to the catalyzed DCPD. All the samples came from the same batch, were the same age, had comparable area fracture planes, and had the same processing conditions. The average max load of the good samples is 42.20 N, which would give a healing efficiency of 122%. The average for the bad samples is 13.17 N which would result in a healing efficiency of 38%. Grouping all those samples together gives an average healing efficiency of

approximately 80%. That compares well to the groundbreaking work by White et. al [14] of 90% healing efficiency for the catalyzed injected DCPD system (albeit for a different specimen geometry) For now the reasoning behind the values for the self-activated system falling into two very different clusters is unknown. Even normalizing for variations in crack surface area still leaves half the samples with 2.5 times as much load held per crack surface area. Because of the higher yield brushing was chosen as the application method for the self-activated samples. It was also assumed that the mechanical force of the brush application could help somewhat to promote dissolution of the wax and therefore might result in increased healing efficiency.

Phase III

Unfortunately, even though self-healing samples were fabricated with embedded wax-encapsulated catalyst and microencapsulated ENB, none of the samples healed enough to provide meaningful data. It was observed visually that after the initial crack event a liquid did wet the crack surface but it evidently did not bond the surfaces together well enough to cause healing. None of the samples developed sufficient strength to give meaningful data. Most of them gave the initial impression that the two halves were bonded together, but after removing the clamps the samples could not even hold their own weight.

2.5 Conclusions

While a good comparison of the healing efficiencies of for different healing agent candidates is not possible with this data set, valuable conclusions can still be drawn with regards to the four healing criteria.

Storage

While the matrix may require the addition of fumed silica to keep the microcapsules and catalyst distributed, such an addition appears to increase the virgin strength.

As seen in other works, these results indicate that wax spheres decrease the virgin strength while microcapsules increase the strength.

Separate from these results casual observations indicate that both the wax encapsulated catalyst and the ENB microcapsules have good shelf lives. Encapsulated catalyst up to one year old has successfully polymerized ENB, while microcapsules as old as 8 months have still shown to be active. These are qualitative results and have not been compared to new materials to compare the effectiveness with time.

Release/Transport

Phase I and II were designed to show a 'best case' scenario for release and transport. Self-activated samples qualitatively showed that the catalyst was being dissolved and thereby released from the wax, but no means of comparing the efficiency of the different healing agents in dissolving the wax to access the catalyst was attempted. Only the Phase III samples could give any indication of the release and transport of ENB into the crack plane. While the max loads did not indicate any significant healing, it was apparent visually that the monomer was filling the crack plane. As the two self-healing faces were pressed back together after initial crack a thin line of shiny liquid was visible in the crack.

Polymerization

The conclusion drawn from the WTDCB testing is that several monomers show better Mode I strength than endo-DCPD. Exo-DCPD showed a moderate increase, while

ENB with and without CL2 showed significant increases both in maximum load and in energy at failure, even at one tenth the catalyst loading. The 3:1 ENB:endo-DCPD blend more than doubled the maximum load and the energy at failure.

By contrast the HTDCB showed endo-DCPD outperforming all others in the Phase I testing. ENB had less than half the value of DCPD. E3D1 was comparable to ENB: well below DCPD. ENB's maximum loads approximately doubled with either a ten-fold increase in catalyst or the addition of 1 wt% Cab-o-sil ©. Phase II indicated that self-activated samples can have good healing efficiency, with better values than the same materials in Phase I.

Another significant conclusion with regards to polymerization is that there is a large amount of scatter inherent in the data.

CHAPTER 3 HEALING OF IMPACT DAMAGE

3.1 Abstract

A major challenge with testing the potential for healing impact damage in composites has been creating an impact event that will cause damage that is likely healable (delamination) without causing too much damage that cannot be healed (fiber breakage). Even a fairly low energy impact event resulting in less than one square centimeter of localized damage (with scattered points of delamination) has very noticeable fiber breakage on the back side. An attempt has been made to use air coupled ultrasound to characterize the damage in the composite, but problems in the equipment prevented us from doing so. It remains to be seen if [when working] the NDE methods will be able to distinguish between cracks and delaminations that have been filled with a healing agent and those that have not.

3.2 Introduction

The second test objective was to evaluate if the same healing mechanism previously demonstrated on Mode 1 failure would be effective in composites suffering impact damage. Adding self-healing ingredients to a FRC means combining all the variables discussed in the healing agent candidate study with those in a standard impact damage of FRC system. Of primary importance are the matrix, the reinforcement, the volume fraction of fibers, microcapsules, and catalyst, and processing conditions. The relevant factors of the impact event include the mass of the rail cart, the height of drop (directly related to the impact

velocity and energy), the diameter of the impactor, the dimensions of the support fixture, the clamping force securing the sample in place.

A number of researchers have looked into the potential benefit of adding toughening particles (usually rubbers or thermoplastics) in between the plies of FRCs, known as interleaving toughening. In general, these particles tend to increase the energy required to cause delamination, either through particulate bridging or simply in causing small-scale redirections of the crack front. Interleaving toughening results in significantly reduced delamination area. Efforts to improve this toughening have shown that a more even distribution throughout the plane results in better toughness. High scatter in the data has so far made it difficult to show an optimum size, shape, or size distribution [61]. Since the microcapsules have been shown to increase toughness in the neat resin system, it is possible that the presence of microcapsules in between plies can have a damage resistant effect, in addition to adding the potential for healing.

The identity of the reinforcement plays a huge role in the behavior and properties of the composite system. Reinforcements are characterized by their composition, the individual fiber thickness, the number of fibers in a tow, whether unidirectional or woven, if woven the style of weave, and how many tows per inch in the warp and weft. The most commonly used continuous reinforcements in structural composites are carbon fibers and glass fibers. For these tests glass fibers provided some significant advantages over carbon or aramid fibers. For a given volume fraction, sample thickness, and impact energy it was assumed that glass fibers would suffer more damage, providing more cracks to potentially heal. The glass fibers provide the additional benefit of being transparent which allows for

visual measurement of overall damage area and potentially healed area. An undamaged composite retains a blurry transparency whereas damage, either delamination or fiber breakage creates a noticeable whitening opacity.

For ease in processing a 12-inch wide plain weave fiberglass tape was selected. The non-adhesive tape was stitched together along the edges, reducing the spread of loose fibers along the minor axis. These fibers were purchased from Fiberglast with 18 tows per inch weft and 17 tows per inch warp.

Many different configurations for the composite provided unsatisfactory results – primarily damage modes that could not be healed. The nature of impact damage and fracture testing typically gives a large amount of scatter to the data, necessitating substantial difference in properties in order to see any statistically significant results. In order to demonstrate healing it was assumed that the damage area would need to be large enough so that a significant portion of the load bearing area would be lost. Ideally an area of sizable delamination with little through-thickness out-of-plane type fiber breakage would occur. Samples with more than four plies exhibited very small damage areas – less than a square inch of area out of a 24 square in panel. Increasing the impact height or weight only served to increase the penetration-type damage without significantly increasing the delamination or damage area. One failed approach consisted of including a layer of woven Kevlar fibers on the top and bottom surfaces of four layers of fiberglass. The thought was that this would allow for increased impact energy and impact damage overall – more to heal – while reducing the amount of out-of-plane damage. In addition to losing most of the transparent advantages by using Kevlar, the impact performance was much poorer. The

yellow Kevlar weave did exhibit a little bit of visually apparent damage – a color difference was noticeable at warp-fill locations where localized delamination had occurred. It was not clear if this cluster of spots represented a number of individual delaminations or one continuous delaminated area. The only configuration that accomplished the goal of a large delamination area without puncture was four layers of fiberglass in a hand lay-up with vacuumed epoxy, pressed in a compression molder at room temperature at 250 psi between two 15”x15”, 1/16” thick aluminum plates.

The necessary impactor setup consisted of the 4.5” x 6.5” composite clamped down with four 200 lbf. toggle clamps in a fixture with a 4 x 6” support area. The impactor mass was the baseline 9.24 lbs of the rail cart without any additional weights, dropped from 8 inches.

A major concern was how to measure the capability of the sample. To accurately assess the healing effectiveness accurate values must exist for the virgin, unimpacted samples, for the impacted samples without healing, and for the healed samples. In this case with three different stages to the healing assessment (injection of catalyzed monomer into simple fiberglass/epoxy system, injection of monomer into system with embedded catalyst – self-activated, and embedded microcapsules and catalyst – self-healing) it is necessary to know the before impact, after impact, and after healing strengths. In the self-healing case the healing begins upon impact and so no testing of impacted but not healed samples was possible.

3.3 Experimental

The composites for the impact tests consisted of the same epoxy (Epon 828 & EpiCure 3223) for the matrix and woven fiberglass fabric for the reinforcement (12-inch plain-weave Woven Fiberglass Tape, Fiberglast).). The four-layer composites were prepared by hand lay-up. For epoxy matrices without catalyst or microcapsules approximately 20 mL of epoxy is required for each layer plus a little extra since some will always remain on the container walls. Epoxy with wax catalyst systems require an additional 5-10 mL of epoxy (apart from the additional volume contributed by the catalyst) for each layer since it cannot be spread as easily and thinly. Approximately 90 mL of epoxy was mixed and placed under vacuum. While the epoxy is under vacuum four 14-inch lengths of fiberglass tape were cut and the base plate prepared. The base plates were 1/16-inch thick aluminum sprayed liberally with PTFE mold release. When the epoxy was sufficiently degassed approximately 20 mL of epoxy was poured onto the first 12- x 14-in sheet arranged on the aluminum plate. A firm plastic squeegee was used to spread the epoxy around until the entire fabric is clearly wetted. Some firmness helps to spread things well but care must be taken not to shift the position of the tows during spreading. After each layer was wetted an Aluminum Bubble Buster roller (Fiberglast) was used to eliminate trapped air by providing a path for the air to escape. . Four layers were laid up in identical fashion. Afterwards the top PTFE-sprayed aluminum plate was placed on top and the entire set up was placed in a compression molder (Model?). The system was placed under 250 psi of compression, which was enough to cause epoxy squeeze-out on all four sides. Some practice samples were cured with the

plates at elevated temperatures, but all of the samples reported were cured at room temperature for 24 hours. After cure the plates usually came off easily. The large composite panels were trimmed to 4.5 x 6.5-inch coupons by the machine shop using a band saw. One 12 x 14-in panel can usually produce five such coupons.

The self-activated system was prepared in the same way with the catalyst stirred into the epoxy after vacuuming. This system is more difficult to spread as some of the wax spheres cluster together. The squeegee can be used to break up these clusters. Because the edges of the fiberglass tape are slightly thicker because they are stitched, as the epoxy squeezes out catalyst and/or microcapsules that were carried by the epoxy tend to build up disproportionally at these edges. These catalyst- and microcapsule-rich areas are part of the normal borders that are trimmed off and discarded. For the self-healing system it is unlikely that the microcapsules would survive the shearing and compression that are part of the normal spreading operation. The microcapsules were applied by pouring microcapsules into a mesh screen and distributing them by hand sprinkling on top of each epoxy/catalyst wetted layer. Because delamination only occurs between layers the total volume of microcapsules was distributed evenly onto only the first three layers with none being placed on the top of the fourth layer. Self-healing samples also did not undergo the de-airing by the Bubble Buster roller to avoid prematurely rupturing more capsules.

The first stage system was carried out as follows. The fiberglass/epoxy composites were subject to drop-weight impact as stated above. The impacted samples were photographed to record the extent of the damage area. DCPD monomer was added to recrystallized 1st Generation Grubbs' catalyst (2.0 mL monomer/mg catalyst) in an ice bath.

Catalyzed DCPD was taken by syringe and injected into the damage area of the composite through either the surface or edge cracks in the impacted composite. In some cases small holes (0.016" diameter) were drilled in the top layer of the damaged region of the composite. This served as a vent hole to allow air displaced by the advancing healing agent an escape route and allowed the healing agent to better fill the cracks and delaminations. The samples were wiped clean on the surface, placed between two 15" x 15" aluminum plates under 50 lbs of load, and allowed to polymerize for 24 hrs at room temperature. In some cases additional air pockets were still visible after the healing time. Additional holes were drilled into these regions that visual inspection indicated that the healing agent had not reached. The before-mentioned visual distinction between damaged and undamaged regions also applied to the healed and non-healed regions, as seen in Figure 17.

Figure 17: Impact Damaged panel with Healing agent injected into left side only

Those areas reached by the healing agent regained their transparency while the healing agent remained a liquid. For cured healing agent, the healed regions were distinguishable both from the undamaged and from the unhealed regions. In many cases the impact event caused delamination across multiple layers. In these instances the healing agent was injected at a certain location between two layers and many times would penetrate all of the layers, but in some cases the gap between two layers would be filled while adjacent gaps between layers would remain open.

For the self-activated system the composite was made as before, but with 5 wt % wax encapsulated catalyst mixed into the epoxy. The system required slightly more epoxy than the simple system in order to fully wet the fibers. After impact and photo documentation, these samples were injected with uncatalyzed DCPD by the same method as listed above. Post injection the composites were compressed locally by either Irwin Quick-Grip® clamps or Bessey plastic spring clamps. Localized clamping allowed for a better closure of the crack plane than did pressing all the samples together under the same set of plates.

Both the plain system with catalyzed monomer and the catalyzed composite system with injected monomer had the twin advantages of an abundance of healing agent and an external driving force (the syringe) to propel the healing agent throughout the crack system. The self-healing system is limited both by the amount of monomer present in the capsules opened by the damage event and by the fact that only capillary action drives the monomer.

The self-healing system required significantly more epoxy to accommodate the wax catalyst and the microcapsules. This increase was caused by the difficulty in spreading the

epoxy system with wax as well as the extra caution required to avoid rupturing the capsules with the shearing incident to spreading the epoxy in the hand lay-up. To further reduce the potential for premature rupture the microcapsules were sprinkled on top of the epoxy-wetted layers 1-3. No capsules were sprinkled on top of the fourth layer as there was no potential for delamination there. Even with the increased epoxy noticeably less epoxy squeezed out during processing. After curing in the compression molder it was visually apparent that some of the microcapsules had broken and had polymerized in the composite. These areas with broken capsules possessed a yellow hue in the affected regions. Panels with broken capsules/polymerized DCPD were sectioned in such a way that the impact site and surrounding areas would contain primarily unbroken capsules. Impacts with the same height and weight as the plain composite system caused damage over a significantly larger area in the self-healing system. Concurrent with the larger damage area was a larger separation between layers. This meant that a smaller amount of healing agent would be required to heal a significantly greater crack volume. Upon applying the clamps at the areas of greatest damage healing agent could be detected visually at the edges (outer ½ in.) of the damage area. This indicates that the microencapsulated healing agent system is viable – the impact event did cause cracks that opened the microcapsules, releasing the healing agent into the crack plane.

Some of the samples were examined by water coupled ultrasound after the impact before injection, and again after the injected healing agent was allowed to cure. The purpose of these scans was to assess if non-destructive testing would be able to detect a difference between the healed and non-healed specimens. If the damaged and healed

areas could be measured quantitatively it would aid in expressing the restoration of properties as a function of healing area. It might also aid in quantitatively comparing healing efficiency of different systems in terms of area healed, whereas a destructive test would be needed to assess mechanical healing efficiency. The system used was a ***??*** using a 2.25 MHz transducer from approximately 1 in away from the sample surface. The critical signal to interpret was the 'B' signal that passes from the transducer through the sample, off the aluminum plate below, back though the sample, and back to the transducer. Air pockets in the composite will not allow much signal to pass through. The greater the damage, the greater the separation between solid layers, the less the signal. In some areas, particularly at the damage edge, even though the damage was visible, the gap between layers did not adequately impede the signal to distinguish between the damaged and the undamaged area. This resulted in slightly smaller damage maps by UT scan than by visual inspection or areas of 'false negative' signal.

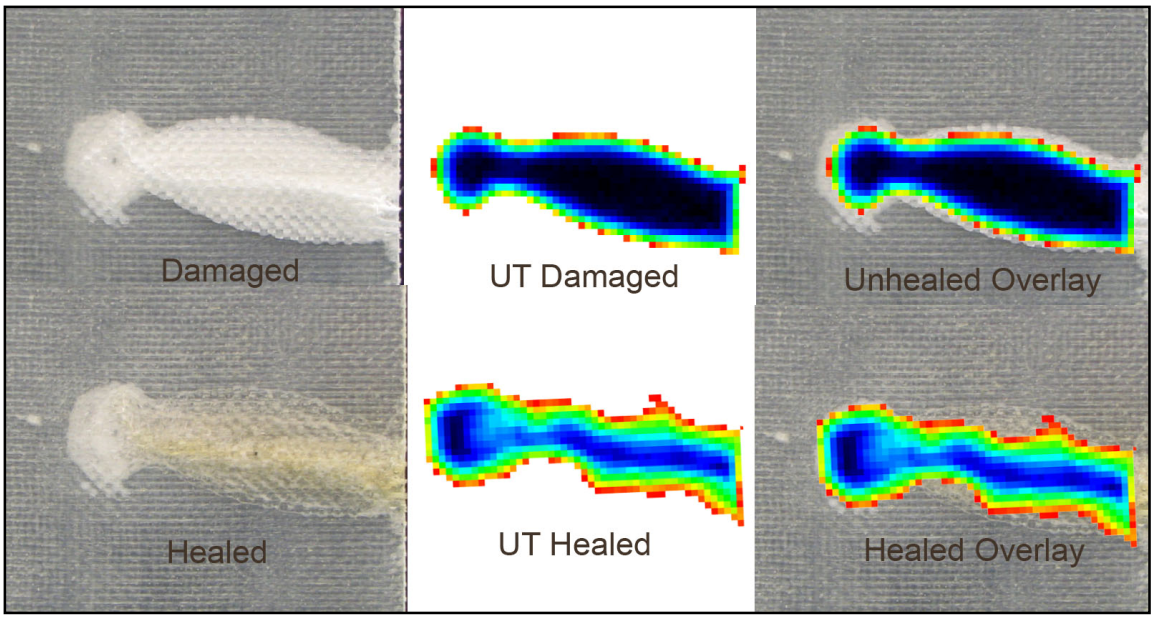

Figure 18: Photograph and Ultrasound image Before and after injection of healing agent

The system was able to accurately map out the damage area for the unhealed composites, but does not give a simple binary damaged or not type result. In the color scheme used an unimpeded signal resulted in saturation and is shown as no color at all, while a slight impedance gave a red/orange/yellow, and increasing signal impedance gave green/light blue/dark blue and finally black where no signal passed through. The images of the healed composites frequently still have regions of dark blue or black (though much smaller than the unhealed). There are two possible explanations for this. First, it is likely that some of the damage areas were non-continuous or did not receive adequate healing agent. Second, some of the healed areas filled a substantial gap between layers and cured, leaving the composite significantly thicker along the major crack area, which could increase the impedance relative to the surrounding regions. Most likely a combination of both

factors explains the remaining dark regions and it is not possible to distinguish from the signal which it might be.

Impact damage typically has a very detrimental effect on a composite's compressive strength. The first attempt to obtain strength measures used a compression-after-impact (CAI) setup wherein the samples are turned vertically, the edges secured to prevent edge buckling, and a compressive load applied to the top edge. A CAI fixture (Boeing Compression After Impact Compression Test Fixture, Wyoming Test Fixtures) was used for these tests. Typically, as the load can no longer be distributed over the entire width due to the impact damage, those areas immediately to either side of the affected region are under an increased stress concentration and suffer a buckling failure. This buckling occurs with either the layers on either side of the delamination moving opposite each other or together with one another as the whole region folds. Because of fixture limitations the samples were trimmed from their impacted size of 4.5 x 6.5 in. to 4 x 6. Unfortunately the impact requirements resulted in samples too thin to withstand the compressive loads adequately. In every case (4-, 8-layer fiberglass, 4-layer fiberglass plus Kevlar, 10-layer carbon fiber) the samples underwent significant out-of-plane buckling, almost always with the upper half of the sample flexing in one direction with the lower half flexing in the opposite direction. The failure mode was almost always a line of crushed material from the right or left edge to the vertical center-line of the composite. This crush line was more commonly near the top or bottom of the composite (Figure 19), but occasionally through the central impacted region. In every case the impact event appeared to be irrelevant to the failure event. Differences in

damage area did not correlate at all to failure load or compressive modulus. Some test batches showed a slight increase in failure load with increase in damage area. To increase the portion of the width affected by the impact event and further highlight the decrease in strength of the damage, some samples were further trimmed slightly along the edges resulting in a sample 3 in wide by 6 in high (i.e. a 1.5 inch damage width affects 37.5% of a 4 in width but 50% of a 3 in width). This had no effect on the failure mechanism. A further attempt was made to decrease the load concentration at the right and left edges by tapering those corners starting a half inch from each end so that the load might be carried more in the impacted region, to enhance the effect of the impact-induced reduction in strength. This also had no effect on the failure mechanism. Further literature reviews showed a wide variety of CAI fixtures with different approaches to prevent the out-of-plane

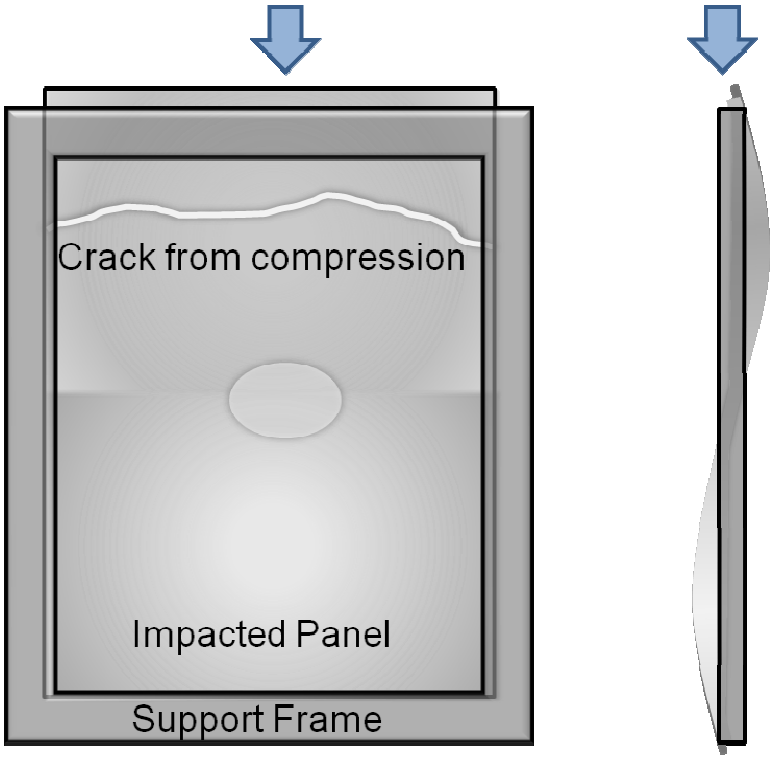

Figure 19: Schematic of typical CAI buckling failure for too-thin samples

bending seen here. This bending rendered the test results meaningless. Other studies in the literature, even those claiming to use 'thin' composites, had a thickness of at least 3 mm. Samples from other studies that suffered similar impact damage did have the failure pass through the impact damage [62][63].

Because edge-wise compression after impact was not possible the samples were tested in a four-point-bend configuration. The interior points were positioned to include the largest damaged area from the greatest number of samples in the area of maximum stress. Crosshead displacement speed was constant at 0.5 inches per minute.

In nearly every case the force bent the specimens into a 'U' shape without suffering any obvious catastrophic failure. Upon removing the load, the composites returned back to their original configuration and were not noticeably weakened. Retesting a specimen showed virtually identical properties, demonstrating that the flexing event did not adversely affect future properties. The results are largely mixed.

For plain composites, without any embedded materials, damaged but unhealed specimens only suffered half as much damage area on average. This makes a direct comparison of properties difficult. There is considerable scatter in the data which also makes it hard to detect trends. Comparing just the average values of maximum flexure load and average damage area (Figure 20) shows an almost perfectly linear relationship. Each additional square cm of damage reduces the maximum flexure load by 10 N. If the relationship between load and damage can be assumed to be linear then the injected healing agent did not improve performance at all. There is one outlier in the data for damaged samples (surrounded by the red dashed circle) that increases the average value by

nearly 100 N. If that data point is excluded then the healed sample performed nearly as well as the damaged samples despite suffering more than twice as much damage. Even amongst just the undamaged specimens, all theoretically equivalent, samples cut from the same panel, some samples are roughly 50% stronger than others (900 vs. 600N).

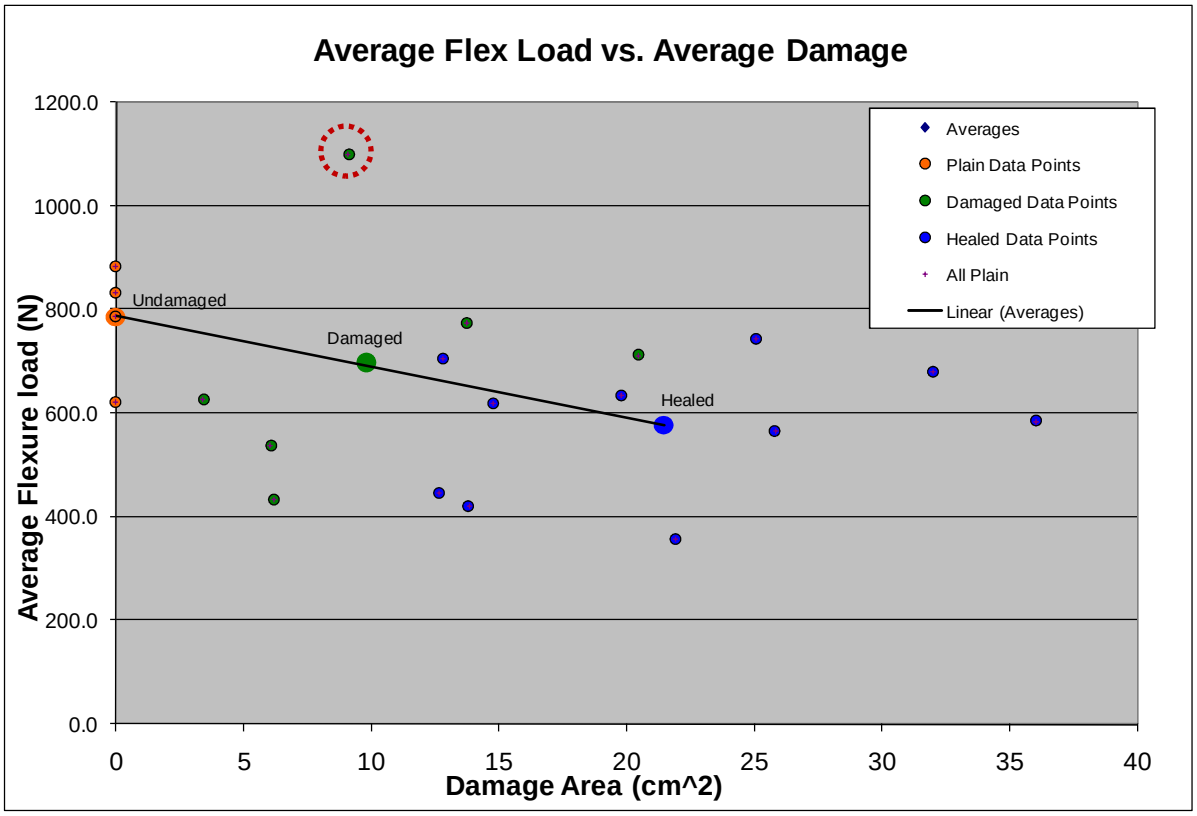

Figure 20: Average flexure load vs. average damage area for plain composites Note the amount of scatter.

3.4 Results and Discussion

For the plain composites in terms of energy required to reach the maximum flexure load the healed samples had a significant increase over the damaged but unhealed specimens (Figure 21) despite having a greater damage area and a somewhat lower load at which that energy was measured. So, even if the injected healing agent did not increase the

strength, it did increase the toughness. As expected, the undamaged specimens averaged a higher energy at maximum flexure load than any of the sample groups that had been damaged. The system with the wax catalyst had approximately the same maximum flexure load and energy at max flexure load for both the damaged and the self-activated samples. These two categories also had very comparable damage areas. Again, as expected the undamaged samples achieved higher loads and required significantly more energy to reach those loads.

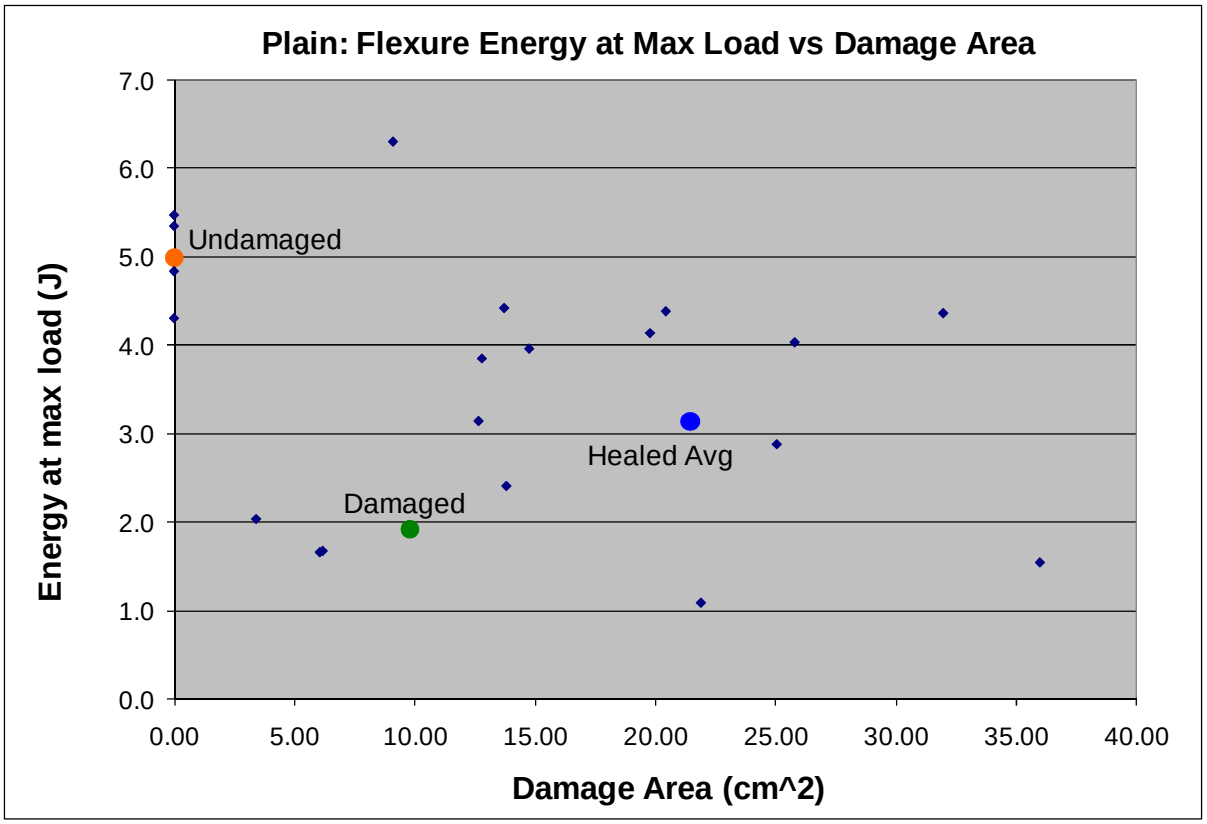

Figure 21: Flexure energy at max load vs. Damage area for plain composites

Comparing flexure modulus of the different groups yields results that at first appear counter intuitive but make sense in the context of the other data. The damaged specimens have a higher modulus than the healed and even the undamaged specimens. Considering

that the damaged but unhealed samples had a comparable maximum flexure load, but had a significantly lower energy to reach that load the area under the curve must be less resulting in a steeper slope and a higher modulus. The self-activated samples indicate the expected results, namely that there was a decrease in modulus from undamaged to damaged, and the injected healing agent restored most of the modulus drop.

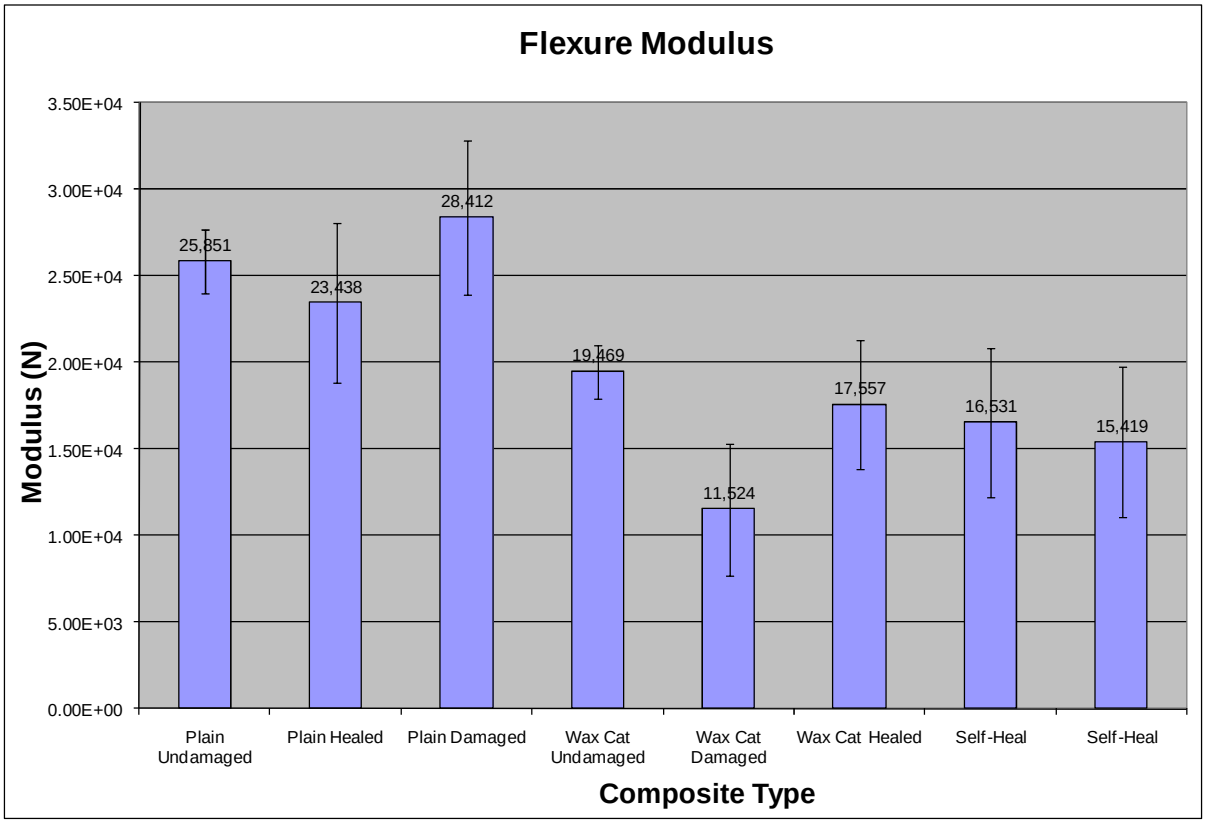

Figure 22: Flexure modulus for all composite groups

The composites containing wax encapsulated catalyst but no microencapsulated healing agent performed more as expected. The undamaged samples containing wax catalyst had a 25 % increase in maximum flexure load over the simple composites. For these the maximum load dropped by almost half from the undamaged to the damaged. The healed samples were only a third less than the undamaged -- roughly 40% more than the

damaged with a very comparable amount of damage (Figure 23). The self-healing samples are also difficult to compare because they either demonstrated almost no damage area or an order of magnitude more damage area. Very few data points for the self healing samples are for samples with comparable amounts of damage as either the plain samples or the samples with wax catalyst. The average of the extreme highs and lows for load and damage area gives a result that would be comparable to the wax damaged and healed values. In general the trend lines for all the different specimens comparing have similar downward slopes showing a decrease in flexure load with increasing damage area.

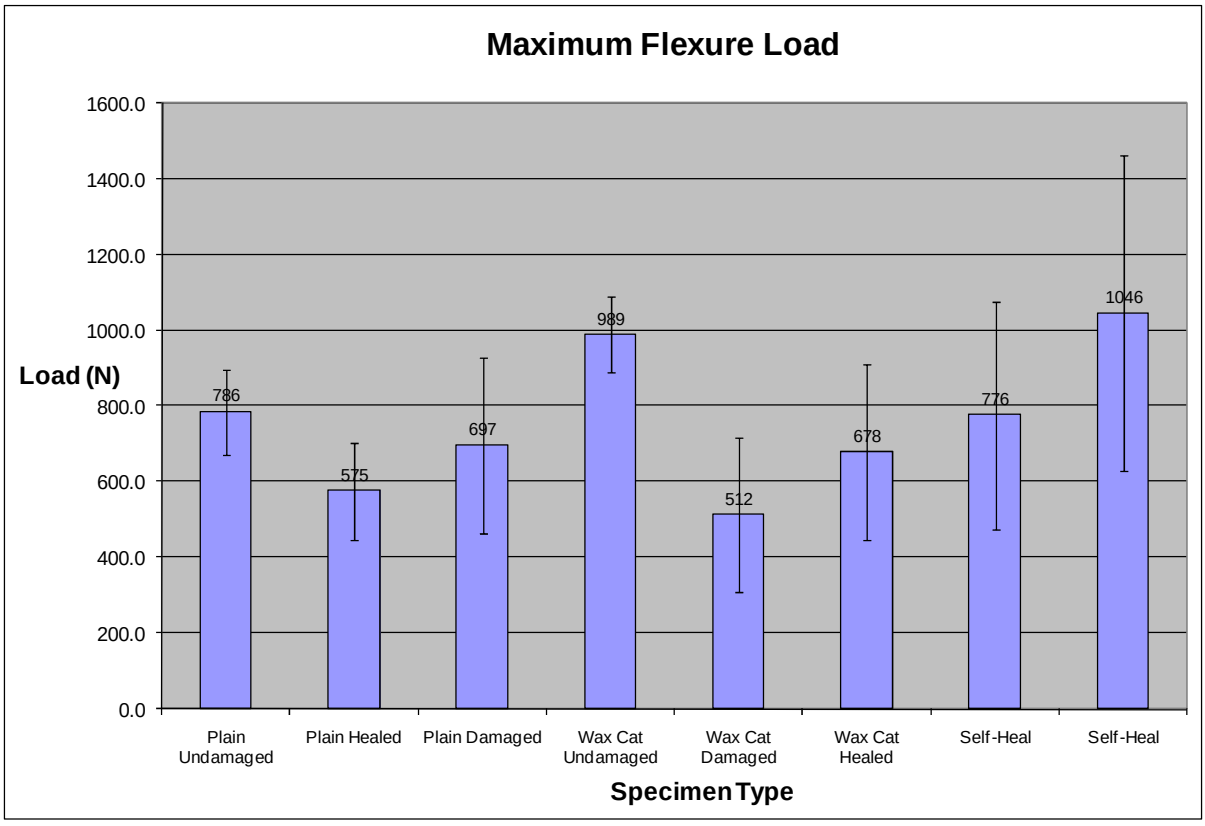

Figure 23: Maximum flexure load for all composite groups

The plot of flexure energy at max load versus damage area is almost identical to the load versus damage but with different 'y' units. Again the healed specimens showed slightly

higher values than the damaged specimens despite a slight increase in damage area. The self healing numbers are either much higher or much lower, but the average is again comparable to the samples containing wax either before or after healing.

3.5 Conclusions

While unable to prove the primary objective of conclusively demonstrating healing in impacted fiber-reinforced composites, several significant lessons may help do so in the future.

Storage

The wax-encapsulated catalyst was successfully stored and processed into this type of composite hand lay-up. Mixing and spreading by squeegee did not render the catalyst ineffective and helped to more evenly distribute it throughout the composite. If desired, the catalyst can even be gathered to give a higher concentration in certain areas. It was visually apparent from the uncut composite panels that microcapsules in some areas remained intact while others ruptured and prematurely polymerized due to the compression molding step.

Release

The self-activated systems did polymerize, demonstrating that the monomer was able to dissolve sufficient catalyst to not leave any liquid monomer still free within the system. The self-healing samples visually showed a successful release of healing agent into the crack plane. Unfortunately it was also visually apparent that the quantity of healing agent released was not nearly sufficient to fill the damage volume. One large panel of

samples looks like a significant portion area has a yellow tint even before impact which would suggest that the bulk of the capsules (or perhaps just the largest ones) ruptured during production (Figure 24). The release is fine; it is the storage through processing that needs to be improved.

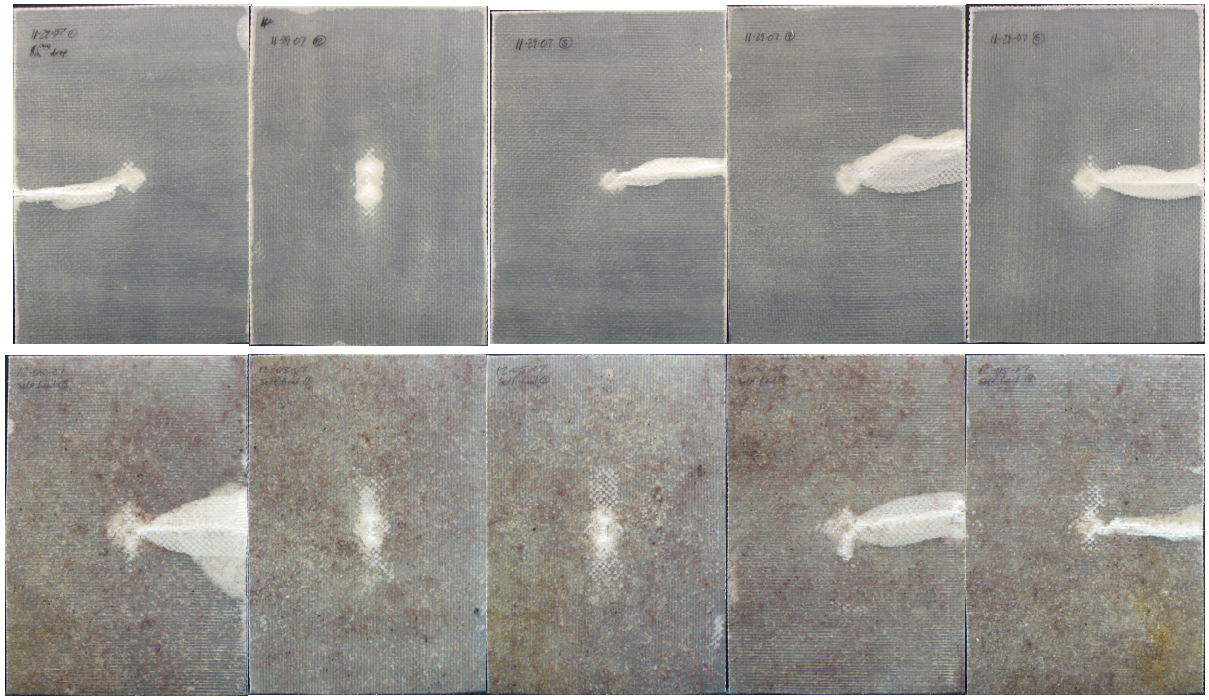

Figure 24: Top: Self-Activated Impacted Panels; Bottom: Self-Healing Impacted panels; Note that purple color comes from catalyst, white speckles come from large microcapsules, and yellow comes from ruptured, polymerized capsules

Transport

Both the injected catalyzed monomer and uncatalyzed monomer successfully moved throughout the damage network, which appeared to be largely interconnected throughout. Thus, it is likely that as long as sufficient healing agent is released, it should be able to flow throughout the extent of the damage. In some samples the injected monomer did not extend all the way to the damage front. Presumably this was not from inadequate driving

force but from air trapped in the composite that could not find a way out. In the idealized self-healing scenario the healing agent would originate from essentially all places at once. This would likely not encounter the problem of a large quantity of liquid healing agent blocking the exit path for trapped air. Indeed in the self-healing systems it was only the area immediately around the crack front that appeared to have liquid healing agent present. In these samples it could easily be seen that as the pressure closing the delaminated plies together increased, thereby decreasing the gap, the liquid spread farther throughout the damage area. Releasing this pressure within five minutes caused the liquid to retreat again until pressure was reapplied.

A system in which the damage could be externally closed more effectively would most likely result in more efficient healing. Alternately, if the damage was more limited to microcracks external forces would probably not be required. Transport of the healing agent worked as well as could be expected.

Polymerization

No aspects of this test were intended specifically to investigate the polymerization. In general, injecting a catalyzed monomer and an uncatalyzed monomer into the damage area did result in a polymer that filled the crack volume. This was to be expected as it was the same system that has been done before. As discussed, the testing method did not give results that could accurately quantify the polymerization. Qualitatively, no monomer either injected or released from a microcapsule remained a liquid so it must have all polymerized or evaporated. The only measure of polymerization from this study was the ultrasonic

imaging, which served to show that the damage volume was no longer empty but now contained a solid.

CONCLUSION: At the same time, a specimen with only minor, micro-sized damage will not have substantially different properties from an undamaged specimen and the difference may be lost in the natural scatter of data. Most likely, a better method of comparison would be some type of fatigue or cyclic loading. Such a system could experience microcrack growth leading to failure at noticeably faster times or lesser loads.

3.6 Acknowledgements

I would like to thank the Army Research Office for their funding of this work.

CHAPTER 4 CHAPTER 4: GENERAL CONCLUSIONS

4.1 General Discussion

While these samples were not able to demonstrate healing, they did give some positive indications that such healing would be feasible. The primary fault in these results lay in the inability to get accurate measurements of the strengths of the composites. As far as could be observed qualitatively, the self-healing aspects of the panels were a success.

Once the impact event happens, most of the damage was interconnected. As long as sufficient healing agent is available, it appears that the DCPD can flow through the composite well and fill up the crack volume. Some amount of air will remain trapped inside as the healing agent seals off the exit routes for the air. In the self-activated system no liquid monomer remained inside the panel. With a wax-encapsulated catalyst loading of 10% (0.5 net wt % catalyst) all the available healing agent in the crack surface polymerized. In the self-healing system it appears that a significant portion of the microcapsules ruptured during processing. They did release the healing agent, which polymerized, but at the wrong time.

While some healing agent was released by the impact event, the damage volume was orders of magnitude larger than the best case volume of healing agent released. The system is well suited to try to heal microcracks or very small-scale delaminations. The system is ill suited to heal large delaminations with any significant volume. To be effective

the microcapsules should be larger in diameter than the crack face displacement – ideally much larger.

The samples were simply too thin to have enough stiffness to give reliable data either in CAI or in 3-point-bend. In CAI even the 8-layer panels failed away from the damage site. Thin 4-layer samples that had been subjected to 3-point-bend forces nearly to the point of folding in half easily came back nearly to their original state. A repeat test on the same sample didn't show any loss in capability from the extensive displacement.

4.2 Recommendations for future research

Several things can be done to improve the existing system to perhaps successfully demonstrate self-healing of impact damage in a fiber-reinforced composite. Primarily, the microencapsulated healing agent system is far better suited to healing microcracks than macro-sized cracks. If a proper sample could be developed to suffer the appropriate damage and a test method found that could distinguish between the undamaged, damaged, and healed panels, self-healing of impact damage could be definitively demonstrated. The real key is finding a test that is sensitive enough to quantify the damage when the damage is merely microcracks. Most likely 12-24 layers would be required to produce a sample that would be stiff enough to fail properly in a CAI setup. A considerable amount of work would be required once a suitable sample had been found to tune the impactor mass and height to produce the amount and type of damage required. Perhaps repeated low-energy impacts would create enough microcracks to be measured. Additional care would need to be taken during fabrication to create more uniform samples. Further investigation into

processing methods that would not prematurely rupture the microcapsules would also be necessary.

References

[1] **Kessler, M. R**., Self-healing: a new paradigm in materials design. *Proc IMechE* Vol. 221 *Part G: J. Aerospace Engineering*.

[2] **Wool, R. P.**, Self-healing materials: a review, *Soft Matter*, **4** (2008).

[3] **Yuan, Y. C., Yin, T., Rong, M. Z.** and **Zhang, M. Q.,** Self healing in polymers and polymer composites. Concepts, realization and outlook: A review. *eXPRESS Polymer Letters*, 2008, Vol. 2, No. 4, 238-250.

[4] **Chen, X., Dam, M. A., Ono, K., Mal, A., Shen, H., Nutt, S. R., Sheran, K, and Wudl, F. A.** Thermally re-mendable cross-linked polymeric material. *Science,* 2002, **295**, 1698-1702.

[5] **Chen, X., Wudl, F., Mal, A. K., Shen, H. and Nutt, S. R.** New thermally remendable highly cross-linked polymeric materials. *Macromolecules*, 2003, **36**, 1802-1807.

[6] **Plaisted, T. A., Nemat-Nasser, S.**, Quantitative evaluation of fracture, healing and re-healing of a reversibly cross-linked polymer, *Acta Materiala*, 2007, **55,** 5684-5696.

[7] **Hayes, S. A., Jones, F. R., Marshiya, K., and Zhang, W.** A self-healing thermosetting composite material. *Compos. A. Appl Sci Manuf.,* 2007*,* **38**(4), 1116-1120.

[8] **Kalista, S. J., Ward, T. C.,** and **Oyetunji, Z**. Self-healing of poly(ethylene-co-methacrylic acid) copolymers following projectile puncture. *Mech. Adv. Mater. Struct.*, 2007, 14:5, 391-397.

[9] **Trask, R. S.,** and **Bond, I. P.** Biomimetic self-healing of advanced composite structures using hollow glass fibres. *Smart Mater. Struct*. 2006, **15**, 704-710.

[10] **Pang, J. W. C.** and **Bond. I. P.** 'Bleeding composites' – damage detection and self-repair using a biomimetic approach. *Compos. A. Appl. Sci. Manuf*., 2005, **36**, 183-188.

[11] **Pang, J. W. C.** and **Bond, I. P**. A hollow fibre reinforced polymer composite encompassing self-healing and enhanced damage visibility. *Compos Sci Technol*. 2005, **65**, 1791-1799.

[12] **Trask, R. S., Williams, H. R.,** and **Bond, I. P**, Self-healing polymer composites: mimicking nature to enhance performance. *Bioinsp. Biomim*., 2007, **2**, 1-9.

[13] **Toohey, K.S., Sottos, N.R., Lewis, J.A., Moore, J.S.,** and **White, S.R**., Self-healing materials with microvascular networks,*Nature Materials*, 2007, **6,** 581-585.

[14] **White, S. R. , Sottos, N. R., Geubelle, P. H., Moore, J. S., Kessler, M. R., Sriram, S. R., Brown E. N,.** and **Viswanathan, S.** Autonomic healing of polymer composites**.** *Nature***,** 2001, **409**, 794-797.

[15] **Schwab, P.**, **France, M. B., Ziller, J. W. and Grubbs, R. H.** A series of well-defined metathesis catalysts – Synthesis of RuCl2(=CHR')(PR3)2 and its reactions. *Angew. Chem. Int. Ed. Engl*., 1995, **34,** 2039-2041.

[16] **Cho, S. H., Andersson, H. M., White, S. R., Sotos, N. R.,** and **Braun, P. V.** Polydimethylsiloxane-based self-healing materials. *Adv Mater*. 2006, **18**, 997-1000.

[17] **Yin, T., Rong, M. Z., Zhang, M. Q.,** and **Yang, G. C.,**Self-healing epoxy composites – Preparation and effect of the healant consisting of microencapsulated epoxy an latent curing agent. *Comp. Sci. Tech*, 2007, **67,** 201-212.

[18] **Brown, E. N., Kessler, M. R., Sottos, N. R.,** and **White, S. R**., In situ poly(urea-formaldehyde) microencapsulation of dicyclopentadiene. *J. Microencapsulation*, 2003, **20**, 719-730.

[19] **Brown, E. N., Sottos, N. R.,** and **White, S. R.** Fracture testing of a self-healing polymer composite. *Expl. Mech.,* 2002, **42** (4), 372-379.

[20] **Rule, J. D., Sottos, N. R.,** and **White, S. R**., Effect of microcapsule size on the performance of self-healing polymers. *Polymer*, 2007, **48,** 3520-3529.

[21] **Blaiszik, B.J., Sottos, N.R.** and **White, S.R.** Nanocapsules for Self-Healing Materials, *Composite Science and Technology,* 2008*,* **68**, 978-986.

[22] **Liu, X.,** and **Lee J. K.,** unpublished results

[23] **Keller, M. W.** and **Sottos., N. R.** Mechanical properties of microcapsules used in a self-healing polymer. *Expl Mech*., 2006, **46**(6), 725-733.

[24] **Kessler, M. R.** *Characterization and performance of a self-healing composite material*. Doctoral Thesis, University of Illinois at Urbana-Champaign, Urbana, IL, 2002.

[25] **Keck, C. G., Kendall, J. L.,** and **Caster, K. C**., Cross-linkers for improved high temperature performance of ROMP adhesives, *Adv. Synth. Catal*. 2007, **349**, 165-174.

[26] **Taber, D. F.** and **Frankowski, K. J.** Grubbs' catalyst in paraffin: an air-stable preparation for alkene metathesis. *J. Org. Chem*., 2003, **68**, 6047-6048.

[27] **Rule, J. D., Brown, E. N., Sottos, N. R., White, S. R.,** and **Moore, J. S.** Wax-protected catalyst microspheres for efficient self-healing materials. *Ad. Mater*., 2005, **17**, 205-208.

[28] **Kessler, M. R.,** and **White, S. R**., Cure kinetics of the ring-opening metathesis polymerization of dicyclopentadiene, *J. Polym. Sci.: A: Polym. Chem*., 2002, **40**, 2373-2383.

[29] **Kessler, M. R., Larin, G. E.,** and **Bernklau, N.,** Cure characterization and viscosity development of ring-opening metathesis polymerized resins. *J. Them. Anal. Calorim.,* 2006, **85**(1), 7-12.

[30] **Rule, J. D.** and **Moore, J. S.** ROMP reactivity of endo- and exo-dicyclopentadiene. *Macromolecules*, 2002, **35**, 7878-7882.

[31] **Larin, G. E., Kessler, M. R., Bernklau, N.,** and **DiCesare, J. C.** Rheokinetics of ring-opening metathesis polymerization of norbornene based monomers intended for self-healing applications. *Polym. Eng. Sci., 2006,* 46*(*12*), 1804-1811*.

[32] **Liu, X., Lee, J. K., Yoon, S. H, Kessler, M. R**., Characterization of diene monomers as healing agents for autonomic damage repair. *J. App. Polym. Sci*., 2006, **101**, 1266-1272.

[33] **Slugovc, C**., The ring opening metathesis polymerization toolbox, *Macromol. Rapid. Commun.*, 2004, **25**, 1283-1297.

[34] **Jones, A. S., Rule, J. D., Moore, J. S., White, S. R., Sottos, N. R.,** Catalyst morphology and dissolution kinetics of self-healing polymers, *Chem. Mater*., 2006, **18**, 1312-1317.

[35] **Stevens, M. P.**, *Polymer Chemistry – an introduction.* 3rd edition, 1999, pp. 253-255 (Oxford University Press, Oxford).

[36] **Kessler, M.R., White, S. R**. Self-activated healing of delamination damage in woven composites. *Compos. A, Appl. Sci. Manuf.* 2001*,* **32,** 683-699.

[37] **Brown, E. N., White, S. R., Sottos, N. R**., Fatigue crack propagation in microcapsule-toughened epoxy. *J. Mater. Sci*., 2006, **41,** 6266-6273.

[38] **Ampudia, J., Larrauri, E., Gil, E. M., Rodriguez, M.,** and **Leon, L. M.**, Thermal scanning rheometric analysis of curing kinetic of an epoxy resin. I. An anhydride as curing agent. *J. App. Polym. Sci*., 1999, **71**, 1239-1245..

[39] **Barbero, E. J.** and **Ford, K. J.**, Characterization of Self-Healing Fiber-Reinforced Polymer-Matrix Composite with Distributed Damage, *Journal of Advanced Materials*, 2007, **39**(4), 20-27.

[40] **Brown, E. N., White, S. R.,** and **Sottos, N. R.** Retardation and repair of fatigue cracks in a microcapsule toughened epoxy composite – Part I: manual infiltration. *Compos. Sci. Technol*., 2005, **65**, 2466-2473.

[41] **Brown, E. N., White, S. R.,** and **Sottos, N. R.** Retardation and repair of fatigue cracks in a microcapsule toughened epoxy composite – Part II: In situ self-healing. *Compos. Sci. Technol*., 2005, **65**, 2474-2480.

[42] **Preghenella, M., Pegoretti, A., Migliaresi, C.**, Thermo-mechanical characterization of fumed silica-epoxy nanocomposites. *Polymer*, 2005, **46**, 12065-12072.

[43] **Beres, W., Koul, A. K.** and **Thamburaj, R.**, A Tapered Double-Cantilever-Beam Specimen Designed for Constant-K Testing at Elevated Temperatures. *Journal of Testing and Evaluation, JTEVA*, 1997, **25**, 536-542.

[44] **Kessler, M. R., Sottos, N.R.,** and **White, S. R**., Self-healing structural composite materials. *Compos. A. Appl. Sci. Manuf*., 2003, **34**, 743-753.

[45] **Blackman, BRK, Hadavinia, H, Kinloch, AJ**, The calculation of adhesive fracture energies in mode I: revisiting the tapered double cantilever beam (TDCB) test. *Eng. Fract. Mech*., 2003, **70**, 233 – 248.

[46] **Lee, J. K., Hong, S. J., Liu, X.,** and **Yoon, S. H.,** Characterization of dicyclopentadiene and 5-ethylidene-2-norbornene as self-healing agents for polymer composite and its microcapsules. *Macromol*. Res., 2004, **12**, 478-483.

[47] **Maudlin, T., Rule, J. D., Sottos, N.R., White, S.R.,** and **Moore, J.S**. Self-healing kinetics and the stereoisomers of dicyclopentadiene. Special Issue of Self-Healing Polymers and Composites, *J. Royal Society: Interface*, 2007, **4**, 389-393.

[48] **Nelson, G. L.** and **Kuo, C.-L.** An improved procedure for the preparation of exo-dicyclopentadiene. *Synthesis*, 1975, **14**, 105-106.

[49] **Liu, X., Lee, J. K., Yoon, S. H.,** and **Kessler, M. R.**, Characterization of diene monomers as healing agents for autonomic damage repair. *J. Appl. Polym. Sci.,* 2006, **101**, 1266-1272.

[50] **Liu, X., Sheng, X., Kessler, M. R.,** and **Lee, J. K.** Isothermal cure characterization of ROMP healing agents for autonomic damage repair: the glass transition temperature and conversion. *J. Them. Anal. Calorim*., 2007, **89**.

[51] **Grela, K.** and **Kim, M.**, A good bargain: An inexpensive, air-stable ruthenium metathesis catalyst derived from α-asarone. *Eur. J. Org. Chem*. 2003, 963-966.

[52] **Kamphaus, J. M., Rule, J. D., Moore, J. S., Sottos, N. R.** and **White, S. R**., A new self-healing epoxy with tungsten (VI) chloride catalyst. *J. R. Soc. Interface*, 2008, **18**.

[53] **Wilson, G.O., Caruso, M.M., Reimer, N.T., White, S.R., Sottos, N.R.** and **Moore, J.S.,** Evaluation of Ruthenium Catalysts for Ring-Opening Metathesis Polymerization-Based Self-Healing Applications, *Chemistry of Materials*, 2008, **20**, 3288-3297.

[54] **Cartie, D. D. R.** and **Irving, P. E.**, Effect of resin and fibre properties on impact and compression after impact performance of CFRP. *Compos. A, Appl. Sci Manuf.,* 2002, **33**, 483-493

[55] **Kumar, C. R. , Radhakrishna, K., Rao, R. M. V. G. K.**, Postcuring Effects on Impact Behavior of Glass/Epoxy Composite Laminates. *Journal of Reinforced Plastics and Composites*, 2005, **24**, 949-959.

[56] **Sanchez-Saez, S., Barbero, E., Zaera, R., and Navarro, C.**, Compression after impact of thin composite laminates. *Comp. Sci. Tech.*, 2005, **65**, 1911-1919.

[57] **Hayes, S. A., Zhang, W., Branthwaite, M.** and **Jones, F. R**., Self-healing of damage in fibre-reinforced polymer-matrix composites. *J. R. Soc. Interface*, 2007, **4**, 381-387.

[58] **Sanada, K., Yasuda, I.** and **Shindo, Y.**, Transverse tensile strength of unidirectional fibre-reinforced polymers and self-healing of interfacial debonding. *Plastics, Rubber and Composites,* 2006, **35**.

[59] **Caprino, G., Lopresto, V., Scarponi, C.,** and **Briotti, G**., Influence of material thickness on the response of carbon-fabric/epoxy panels to low velocity impact. *Comp. Sci. Tech.*, 1999, **59**, 2279-2286.

[60] **Naik, N. K., Joglekar, M. N., Arya, H., Borade, S. V.** and **Ramakrishna, K. N**.,. Impact and compression after impact characterization of plain weave fabric composites: effect of plate thickness. *Adv. Composite Mater.,* 2004*,***12**, 261-280.

[61] **Derkowski, B. J.,** and **Sue, H. J**., Morphology and compression-after-impact strength releationship in interleaved toughened composites. *Poly. Comp.*, 2003, **24**, 158-170.

[62] **De Freitas, M., Reis, L**., Failure mechanisms on composite specimens subjected to compression after impact. *Composite Structures*, 1998, **42**, 365-373.

[63] **Khondker, O. A., Leong, K. H., Herszberg, I.** and **Hamanda, H**., Impact and compression-after-impact performance of weft-knitted glass textile composites. *Compos. A, Appl. Sci Manuf.,* 2005, **36**, 638-648.

[64] **Kan H. P**. Enhanced reliability prediction methodology for impact damaged composite structures. Report DOT/FAA/AR-97-79, October 1998.

[65] **Kumar, C. R. , Radhakrishna, K., Rao, R. M. V. G. K.**, Postcuring Effects on Impact Behavior of Glass/Epoxy Composite Laminates, *Journal of Reinforced Plastics and Composites* 2005, **24**, 949-959.

[66] **Caprino, G., Langella, A.,** and **Lopresto, V.,** Indentation and penetration of carbon fibre reinforced plastic laminates. *Compos. B, Engr.,* 2003, **34**, 319-325.

[67] **Caprino, G.** and **Lopresto, V**., On the penetration energy for fibre-reinforced plastics under low-velocity impact conditions. *Comp. Sci. Tech*., 2001, **61**, 65-73.

[68] **Gustin, J., Freeman, B., Stone, J., Mahinfalah, M.,** and **Salehi-Khojin**, A., Low-velocity impact of nanocomposite and polymer plates. *J. Appl, Polym. Sci*., 2005, **96**, 2309-2315.

[69] **Kuang, K. S. C,** and **Cantwell, W. J**., Detection of impact damage in thermoplastic-based glass fiber composites using embedded optical fiber sensors. J. Thermoplastic Compos. Mater., 2003, **16**, 213-223.